A Line Outage Study for Prediction of Static Power Flow Redistribution

By

Nan Wei

Thesis submitted to the faculty of the

Virginia Polytechnic Institute and State University

In partial fulfillment of the requirements for the degree of

Master of Science

In

Electrical Engineering

Jaime De La Ree Lopez

Virgilio A. Centeno

Vassilis Kekatos

August 12, 2016

Blacksburg, Virginia

Keywords: Transmission Line Outage, Contingency Analysis, Power Flow Redistribution, Line Outage Distribution Factor, Thevenin Equivalent Electrical Distance

Abstract

Transmission line is a crucial role in power transmission network which connects generating units to consumers. Some unpredicted failure events such as lightening or system faults can cause transmission line tripped, which may bring about a large interruption to the system and causes damage. When line outage happens, the power flow on the tripped line will be redistributed to the rest of lines in the system. It may cause risk of overload happens on other lines, and results in a cascading failure and system collapse. Reasonably, a single line outage will not affect all other lines in the system. Therefore, when a line outage happens, it is important for the system operator to have a preview of which lines will have serious impact and which lines will not, so that the operator can only focus on monitoring certain lines which will be seriously affected, rather than keeping monitoring the whole system. In this thesis, A Line Outage Distribution Factor (LODF) method is proposed and implemented in the IEEE 118 bus system to estimate active power flow redistribution after a line outage. After that, a definition of Thevenin electrical distance between two transmission lines is derived and applied to calculate electrical distances between the outage line and each line in the system. An exponential convergence tendency is found between maximum possible LODF predicted power flow variations and electrical distance, and an exponential regression method is applied to analyze this tendency. The contribution of this work is a rule has been found that starting from the outage line, the maximum possible active power flow variation on transmission lines exponentially decreases exponentially while the electrical distance increases. With only the information of system's normal operating condition and topological information, the maximum possible active power change on each lines caused by single line outage, and the margin of the impact of single line outage on power flow variations may propagate along electrical distance can be easily and quickly predicted. Ultimately, the goal of this work is to allow operators at the control center can concentrate on lines within a certain electrical distance instead of keeping monitoring the whole system when a line outage happens.

Acknowledgement

I would like to express my sincere gratitude to my advisor, Dr. Jaime De La Ree Lopez, for his encouragement, patience, and motivation throughout my two-year master study. He has provided me many precious ideas and best support on my work when I feel confused. He has also brought his kindness and friendship to my life. I feel really grateful for all of these. As my committee members I would also like to thank Dr. Virgilio. A. Centeno and Dr. Vassilis Kekatos for their patience and support to my study.

I wish to thank my great lab-mates in the power group. They offers me all they can to help me with my research. To Jacques and Andreas, I want to thank you for so many times you came to me with plenty of great ideas and your help with my English expression.

Finally, I would like to bring my deepest thanks to my parents, Xuan Wei and Hongye Ren, and also to my girlfriend, Jiaxin Zhu. They have been giving me their best love and encouragement throughout my life.

Table of Contents

List of Figures

List of Tables

Chapter 1: Introduction and literature review

1.1 Introduction and Literature Review

Transmission lines are essential links in a power transmission network which connects generating units to consumers. The fact that they are exposed to atmospheric conditions and always cover a long geographic distance increases the risk of system faults or contingencies. When a contingency occurs on a transmission line, appropriate circuit breakers on it have to be tripped to isolate the damage and to protect the rest of the system resulting in a transmission line outage. When a line outage occurs, the system has to find a new equilibrium point. The operating condition of system will change, and the power flowing on the tripped line will be redistributed to the rest of the lines in the system. The upcoming voltage and current transients will fall off soon, and the system will reach a new steady-state. Since the power on the outage line will be redistributed to the other lines in the system, it is possible for some lines in the system to become overloaded and subsequently tripped. These line failures may cause more electric components to perform abnormally and be tripped. In this case, a vicious cycle or cascading events will be generated resulting in the removal of more electrical components from the system. This cascading failure may expand over a large area of the network resulting in serious system and consequently economic damage. Several historical blackouts have been documented to support this phenomenon.

On March 11, 1999, in southern Brazil, a large blackout happened in the three largest cities which resulted in 170 million people stranded in darkness for about two hours. This disaster started with a lightning strike at a substation leading to the outage of most of the 440kV transmission lines connected to the substation in Bauru. Many plants automatically shut down as a result of the poor connecting conditions between the plants and the transmission network. The removal of several plants and High-Voltage lines (440 kV) forced other portions of the network to try to support the connected load.

These conditions created overloaded lines in other sections of the system and the disconnection of additional elements. A chain reaction of line and generator disconnections forced the system into a complete collapse [1].

On August 14, 2003, the northeastern part of the USA experienced the world's second most widespread blackout in history. More than 55 million people in eight states across the US were affected. It took a week to restore all the power system. The blackout started from an incorrect action on a monitoring tool. Afterwards, several 345kV overhead transmission lines failed due to tree faults while the alarm system failed to act. With the power shift by the first line failure, several 345kV power lines and 138 kV lines overloaded and failed soon after that [2].

On November 4, 2006, more than 15 million people did not have access to electricity for two hours in major part of Europe. The reason for this large blackout was a planned routine line disconnection without communicating to the neighboring operating center. Eventually, the disconnection caused a high power flow on neighboring transmission lines and led to a cascading line failures [3].

All three examples illustrate the serious consequences of a cascading line contingency. To solve this situation, it is important for the control center to evaluate how the power flows will change after the occurrence of the first line outage so that the operator can respond and take correct actions in time to avoid any following outages (cascading failures) [4].

Up to now, plenty of research topics on line outage contingency analysis have been discussed such as line outage detection and identification methods in power system transmission networks [5-13], analysis of cascading line failures [14-17], sensitivity factors analysis method [18], and analysis of line outages for secure voltage operation [19-22].

In this work, an estimation of the steady-state effect of a single line outage in the system is accomplished by the Line Outage Distribution Factor (LODF) algorithm. LODF gives the change of active power flow on each line in the system due to a single line outage. Due to Kirchoff voltage and current laws, the further the electrical distance

of a line from an outage is, the less effect that line will see. A line outage that happens should have small or negligible effect on the active power change on distant lines. To quantify the distance between the outage line and other lines in the system, a definition of a Thevenin equivalent electrical distance between two transmission lines is derived. The IEEE 118 bus system is selected to perform the LODF and electrical distance algorithms and observe the relationship between power change on all lines and electrical distance as it is large enough to observe the margin of impact of line outages on power flow redistribution. An exponential convergence tendency is observed between the maximum possible active power flow variation on lines and electrical distances from the outage line to other lines in the system.

1.2 Thesis Outline

Chapter 1 provides a brief introduction and motivation to conduct this line outage contingency analysis research. Chapter 2 reviews some background knowledge of power systems and detailed derivation of some power system concepts and parameters which will be mentioned in chapter 3. Chapter 3 demonstrates the detailed analysis of the steady-state impact of line outages on voltage angle changes and power flow variations in the IEEE 118 bus system. A regression method has been used to compare power flow redistributions to electrical distances due to the impact of line outages. Chapter 4 concludes the work and gives a future scope of work.

Chapter 2: Background knowledge

This chapter presents some basic power system knowledge and mathematical models that are mentioned in the later chapters.

2.1 Power System Steady-State Analysis

The steady state stability of a power system is defined as the ability of the system to return to steady state following a small disturbance [23]. Power systems bear a great deal of disturbance at all times, such as small variations of loads in a system and subtle changes of distance between parallel overhead transmission lines cables caused by wind, which will affect line impedance.

In steady-state analyses, systems are assumed to be under three-phase balanced operation condition and the total generation always matches the total loads in the system. Therefore, systems in this analysis are simplified as single phase per unit system.

2.2 Bus Admittance Matrix and Bus-Impedance Matrix

For an n buses system, the bus admittance matrix or the Y_{bus} is an $n \times n$ matrix that shows the relationship between nodal current injection and nodal voltage in the system.

$$I=Y_{bus}V \tag{2.2.1}$$

$$Y_{bus} = \begin{bmatrix} Y_{11} & Y_{12} & \cdots & Y_{1n} \\ Y_{21} & Y_{22} & \cdots & Y_{2n} \\ \vdots & \vdots & \ddots & \vdots \\ Y_{n1} & Y_{n2} & \cdots & Y_{nn} \end{bmatrix} \quad (2.2.2)$$

I is an n × 1 vector which contains current injections on all nodes, from bus 1 to bus n whereas V is an n × 1 vector contains voltage phasors refer to ground on all buses.

The diagonal element, Y_{jj}, in Y_{bus} is the self-admittance of bus j. It is equal to the sum of the admittance of all transmission lines, transformers, and capacities connected to bus j. The off-diagonal element, Y_{jk}, is the transfer admittance between bus j and bus k, which equals to the negative value of admittance of lines, transformers, and capacities connected between bus j and bus k. If there is no connection between bus j and bus k, Y_{jk} is equal to zero. For a large scale power system with thousands of buses, Y_{bus} is a symmetrical and sparse matrix that most elements in it are zeros. It shows the topology of the network.

The bus impedance matrix, or Z_{bus} shows the relationship between the nodal voltage and the nodal current injection in the system. Generally, the calculation of Z_{bus} is equal to the inverse of Y_{bus} .

$$V = Z_{bus} I \quad (2.2.3)$$

The diagonal element, Z_{jj}, in Z_{bus} is the self-impedance or driving impedance of bus j whereas the off-diagonal element, Z_{jk}, is the transfer impedance between bus j and bus k. Unlike Y_{bus} matrix, Zbus is a full matrix whose elements cannot be calculated separately. There is no direct relation between elements in Y_{bus} and Z_{bus}. Z_{jk} is equal to V_j / I_k when all other buses are open circuit while Y_{jk} is equal to V_j / I_k when all other buses are short circuit.

In real life, sometimes the system is too large with more than 50000+ buses to calculate Z_{bus} matrix by inverting Y_{bus}. However, a Z_{bus} building algorithm can be utilized to calculate Z_{bus} matrix.

Practically, Y_{bus} is usually used in power flow problem. Since power flow problems involve an iterative solution, the sparsity of Y_{bus} make it more efficient to solve the problem. In comparison, Z_{bus} is usually used in fault analysis because each element in Z_{bus} represents the relationship between node voltage and node current injection when there is only one non-zero current injection which corresponds to the faulted bus. Therefore, all bus voltages can be acquired with only one current injection. If this current is fault current, all bus voltages will be easily calculated and then, the system state variables in fault situation are also accessible.

2.3 Electrical Distance

The concept of electrical distance was first proposed by Lagonotte P in the application of reactive power control [24], which was used to express the electrical coupling between buses. Until now, several methods have been developed to express electrical distance but there is no consensus yet. The existing methods are divided into two categories: sensitivity method and impedance method. This section discusses a method purposed in [25] which uses Thevenin impedance between two nodes to indicate the electrical distance between them.

When a network with N buses is energized by current injections ΔI_j on bus j and ΔI_k on bus k, the changes in voltages on all buses can be obtained as follows:

$$\begin{bmatrix} \Delta V_1 \\ \vdots \\ \Delta V_j \\ \Delta V_k \\ \vdots \\ \Delta V_N \end{bmatrix} = \begin{matrix} ① \\ \\ ⓙ \\ ⓚ \\ \\ Ⓝ \end{matrix} \begin{bmatrix} Z_{11} & \cdots & Z_{1j} & Z_{1k} & \cdots & Z_{1N} \\ \vdots & \ddots & \vdots & \vdots & \ddots & \vdots \\ Z_{j1} & \cdots & Z_{jj} & Z_{jk} & \cdots & Z_{jN} \\ Z_{k1} & \cdots & Z_{kj} & Z_{kk} & \cdots & Z_{kN} \\ \vdots & \ddots & \vdots & \vdots & \ddots & \vdots \\ Z_{N1} & \cdots & Z_{Nj} & Z_{Nk} & \cdots & Z_{NN} \end{bmatrix} \begin{bmatrix} 0 \\ \vdots \\ \Delta I_j \\ \Delta I_k \\ \vdots \\ 0 \end{bmatrix} = \begin{bmatrix} Z_{1j}\Delta I_j + Z_{1k}\Delta I_k \\ \vdots \\ Z_{jj}\Delta I_j + Z_{jk}\Delta I_k \\ Z_{kj}\Delta I_j + Z_{kk}\Delta I_k \\ \vdots \\ Z_{Nj}\Delta I_j + Z_{Nk}\Delta I_k \end{bmatrix} \quad (2.3.1)$$

Where

Z_{jk}= transfer impedance between bus j and bus k

Z_{kk}= driving impedance of bus k

Adding the voltage changes on bus i and bus k to get the final voltages on bus i and bus k:

$$V_j = V_j^0 + Z_{jj}\Delta I_j + Z_{jk}\Delta I_k \quad (2.3.2)$$

$$V_k = V_k^0 + Z_{kj}\Delta I_j + Z_{kk}\Delta I_k \quad (2.3.3)$$

Where V_j^0 and V_k^0 are the voltage phasors on bus j and bus k before two current injections were engaged.

Adding and subtracting $Z_{jk}\Delta I_j$ in (2.3.2) and $Z_{jk}\Delta I_k$ in (2.2.3):

$$V_j = V_j^0 + (Z_{jj} - Z_{jk})\Delta I_j + Z_{jk}(\Delta I_j + \Delta I_k) \quad (2.3.4)$$

$$V_k = V_k^0 + Z_{jk}(\Delta I_j + \Delta I_k) + (Z_{kk} - Z_{kj})\Delta I_k \quad (2.3.5)$$

Since Z_{bus} is a symmetrical matrix, Z_{kj} is equal to Z_{jk}. Equation (2.3.4) and (2.3.5) indicates the Thevenin equivalent circuit between two buses. The open-circuit voltage between them is:

$$V_{oc,kj} = V_k^0 - V_j^0 \quad (2.3.6)$$

The Thevenin equivalent circuit between bus j and bus k can be deduced from equation (2.3.4) and (2.3.5) as follows:

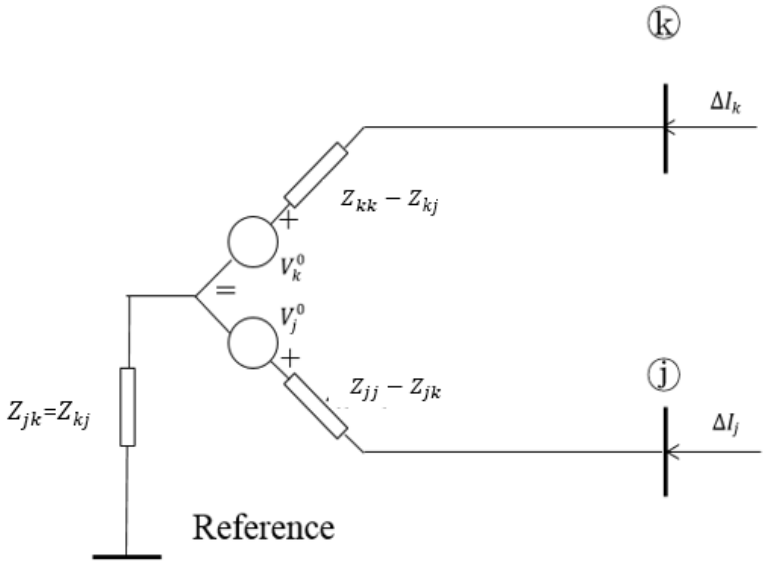

Figure 2. 1: Thevenin equivalent circuit between bus j and bus k

The short circuit current between them is:

$$\mathrm{I}_{sc,kj} = \Delta \mathrm{I}_j = -\Delta \mathrm{I}_k = (V_k^0 - V_j^0)/(Z_{jj} - Z_{jk} + Z_{kk} - Z_{kj}) \quad (2.3.7)$$

Therefore, the Thevenin impedance between bus j and bus k is:

$$Z_{th,jk} = \frac{\mathrm{V}_{oc,kj}}{\mathrm{I}_{sc,kj}} = Z_{jj} + Z_{kk} - 2Z_{jk} \quad (2.3.8)$$

The author in [25] proposed that the mutual electrical distance between node j and node k is equal to the Thevenin impedance between them. This implies that a large value of Z_{jk} represents a closer mutual electrical distance and a strong coupling between two nodes (the value of Z_{jk} is always smaller than the values of Z_{jj} and Z_{kk}).

2.4 Load Flow Analysis

Load flow (power flow) is a useful power system steady-state analysis method. In a network, with system topology, power generations, and power consumptions given, this analysis method can be used to calculate voltage magnitudes and angles on all buses as well as the real and reactive power distribution in the network.

This section introduces the derivation of a full AC Newton-Raphson load flow method, which plays a key role to obtain the accurate system state. Also, DC power flow method is also discussed as an approximation of NR method that is usually used to estimate the relationship between system state variables.

2.4.1 Basic Load Flow Formulation

In load flow analysis method, an assumption can be made that systems are operated under three-phase balanced operation condition, which allows a single-phase representation of the system. The loads are assumed to be constant during calculation.

For an n buses system network, the relationship between current injection on bus i and voltage on bus i can be derived using equation (2.2.1):

$$\mathrm{I}_i = \sum_{k=1}^{n} \mathrm{Y}_{ik}\mathrm{V}_k \qquad i = 1,2 \ldots, \mathrm{n} \qquad (2.4.1.1)$$

Where

I_i= Phasor of current injections on bus i.

V_i= Phasor of current injections on bus i.

Y_{ik}= The element in ith row and kth column in $\mathrm{Y}_{\mathrm{bus}}$.

Equation (2.4.1) is a linear problem if the current injections are given. However, it is not the real case. In practice, the current injections on most buses are unspecified. The relation between current injection and P, Q, and V at any bus i is shown as:

$$\mathrm{I}_i = (\mathrm{P}_i - j\mathrm{Q}_i)/\mathrm{V}_i^{*} \qquad (2.4.1.2)$$

In an n bus system network, there are three kinds of buses:

(1) Slack bus (Swing bus): Voltage magnitude is one per unit and phase angle stay at zero all the time. This bus is assumed connected to an ideal infinite large generator, its real and reactive power outputs are decided by the rest of system. It is used to keep balance of total power generation and total power consumption in the whole network. In a general way, bus 1 is slack bus in a network. Sometimes, a decent limit will be chosen for reactive power output Q to make it in a reasonable range. Otherwise, the power flow solution could be impractical.

(2) Voltage-controlled bus (PV bus): Real power and voltage magnitude on bus are given and constant. Generally, all the generator buss except slack bus are PV bus. (unless the unit reaches maximum excitation and then it becomes PQ as no further voltage support can be provided)

(3) Load bus (PQ bus): Real power and reactive power on bus are given and constant. Load is assumed to be constant.

For different types of buses, the given conditions are varied, which make the problem nonlinear. Then the power injections on bus i is:

$$\begin{aligned} S_i &= V_i I_i^* \\ &= V_i (\sum_{k=1}^{n} Y_{ik} V_k)^* \\ &= V_i \sum_{k=1}^{n} Y_{ik}^* V_k^* \quad i = 1,2 \dots, n \end{aligned} \tag{2.4.1.3}$$

The Bus admittance matrix, Y_{bus}, can be divided into two sub-matrices, bus conductance matrix G and bus susceptance matrix B. The elements of these sub-matrices can be added to obtain the original matrix element as follows:

$$Y_{ik} = G_{ik} + jB_{ik} \tag{2.4.1.4}$$

Therefore,

$$S_i = \sum_{k=1}^{n} |V_i||V_k| e^{j\theta_{ik}} (G_{ik} - jB_{ik})$$

$$= \sum_{k=1}^{n} |V_i||V_k| (cos\theta_{ik} + jsin\theta_{ik})(G_{ik} - jB_{ik}) \quad i = 1,2 \dots, n \tag{2.4.1.5}$$

where $\theta_{ik} = \theta_i - \theta_k$. θ_i is the voltage angle on bus i, and θ_k is voltage angle on bus k.

Dividing equation (2.4.1.5) into real and imaginary parts, the real power injection and reactive power injection into bus i can be formulated as:

$$P_i = \sum_{k=1}^{n} |V_i||V_k| (G_{ik} cos\theta_{ik} + B_{ik} sin\theta_{ik}) \tag{2.4.1.6}$$

$$Q_i = \sum_{k=1}^{n} |V_i||V_k| (G_{ik} sin\theta_{ik} - B_{ik} cos\theta_{ik}) \tag{2.4.1.7}$$

Assuming the number of load busses in this n bus network is b, the real power injections on all PV buses and all PQ buses are given to be P_{net} and the reactive power injections on all PQ buses are given as Q_{net}.

Formulating the power flow equations into the form of f(x) = 0, where x is the state of system. It contains voltage magnitudes of all load buses, and voltage angles on all buses except slack bus. The power flow equations may be reformed to:

$$f_i^P = \mathrm{G}_{ii}|\mathrm{V}_i|^2 + |\mathrm{V}_i| \sum_{k=1}^{n} |\mathrm{V}_k|(\mathrm{G}_{ik}\cos(\theta_i - \theta_k) + \mathrm{B}_{ik}\sin(\theta_i - \theta_k)) - \mathrm{P}_{neti} = 0 \quad (2.4.1.8)$$

$$f_i^Q = \mathrm{B}_{ii}|\mathrm{V}_i|^2 + |\mathrm{V}_i| \sum_{k=1}^{n} |\mathrm{V}_k|(\mathrm{G}_{ik}\sin(\theta_i - \theta_k) - \mathrm{B}_{ik}\cos(\theta_i - \theta_k)) - \mathrm{Q}_{neti} = 0 \quad (2.4.1.9)$$

For this n buses system network with b load buses, an equations set with *n-1* equations of (2.4.1.8) and b equations of (2.4.1.9) can be generated.

To solve this nonlinear power flow equations sets, two iterative techniques are commonly used: Gauss-Seidel and Newton-Raphson iteration method. Compared with Newton-Raphson method, Gauss-Seidel method is simpler and consumes less time in computation. However, for a larger system, Gauss-Seidel will take more iterations and more time to converge. Therefore, in practice, Newton-Raphson is mainly used to solve power flow problems.

In this section, Newton-Raphson method is reviewed which is relevant to the material in the next chapter. The detailed derivation of Gauss-Seidel method is provided in reference [26].

2.4.2 Newton-Raphson (N-R) Iteration Method

Compared with Gauss-Seidel iteration, Newton-Raphson is a more sophisticated method to calculate load flow solutions and both the calculation time and iteration time are smaller to converge. Also, the scale of system will not increase its iteration time. N-R iteration method is derived from the Taylor series expansions for $f(x + \Delta x)$ at an estimated initial condition of state vector x. The higher order terms of it are ignored. Therefore, the equation becomes:

$$f(x + \Delta x) \cong f(x) + f'(x)\Delta x \quad (2.4.2.1)$$

This formulation makes a linear approximation between small changes in state vector and small changes in f(x). If the dimension of x is n, the structure of (2.4.2.1) is:

$$\begin{bmatrix}\Delta f_1(x)\\ \vdots \\ \Delta f_n(x)\end{bmatrix} = \begin{bmatrix}\frac{\partial f_1(x)}{\partial x_1} & \cdots & \frac{\partial f_1(x)}{\partial x_n}\\ \vdots & \ddots & \vdots \\ \frac{\partial f_n(x)}{\partial x_1} & \cdots & \frac{\partial f_n(x)}{\partial x_n}\end{bmatrix} * \begin{bmatrix}\Delta x_1\\ \vdots \\ \Delta x_n\end{bmatrix} \qquad (2.4.2.2)$$

For the power flow problem, the derivative $f'(x)$ is known as Jacobian matrix. The state vector, *x*, contains voltage magnitude $|V|$ for all *PQ* buses and voltage angle θ for all buses except the slack bus. $f(x)$ includes real power injection *P* for all buses except the slack bus and reactive power injection Q for all *PQ* buses. The equation becomes:

$$\Delta f(x) = \begin{bmatrix}\Delta P\\ \Delta Q\end{bmatrix} = J(x) * \Delta x = \begin{bmatrix}\frac{\partial P}{\partial \theta} & \frac{\partial P}{\partial |V|}\\ \frac{\partial Q}{\partial \theta} & \frac{\partial Q}{\partial |V|}\end{bmatrix} * \begin{bmatrix}\Delta \theta\\ \Delta |V|\end{bmatrix} \qquad (2.4.2.3)$$

When solving the power flow problem, a more general N-R iteration formula will be used:

$$x^{v+1} = x^v + \Delta x^v = x^v - [J(x^v)]^{-1} f(x^v) \qquad (2.4.2.4)$$

Where *v* is the iteration index. As an initial condition of state vector is chosen to be x^1 , using equation (2.4.2.4) to calculate $x^2 = x^1 + \Delta x^1$. Keeping running the iteration until the difference between x^{v+1} and x^v are negligible. Then, x^v is the load flow solution.

In this work, Newton-Raphson power flow method is used to compute the basic operation condition of the system. However, since Newton-Raphson is an iteration method, it is difficult to dig out the direct relationship between the state vector x and f(x). Therefore, the derivation of DC power flow method, a linear approximation of Newton-Raphson power flow method, is presented in the next section.

2.4.3 DC load Flow

To derive DC load flow model, the first step is to make an approximation of Newton-Raphson method to decoupled power flow method. The derivation of this method is proposed in [27].

In a typical power system, the reactance of transmission line is much greater than the resistance of it, which leads to a weak coupling between *P* and *V* and also between *Q*

and θ. Thus, the coupling submatrices $\frac{\partial P}{\partial |V|}$ and $\frac{\partial Q}{\partial \theta}$ in Jacobian matrix can be neglected.

Then, the power flow equation becomes:

$$\frac{\partial P_i}{\partial \theta_k} = |V_i||V_k|(G_{ik}sin\theta_{ik} - B_{ik}cos\theta_{ik}) \quad (2.4.3.1)$$

$$\frac{\partial P_i}{\partial \theta_i} = -Q_i - B_{ii}|V_i|^2 \quad (2.4.3.2)$$

$$\frac{\partial Q_i}{\partial |V_k|} = |V_i|(G_{ik}sin\theta_{ik} - B_{ik}cos\theta_{ik}) \quad (2.4.3.3)$$

$$\frac{\partial Q_i}{\partial |V_i|} = \frac{Q_i}{|V_i|} - B_{ii}|V_i| \quad (2.4.3.4)$$

To simplify the problem, a further approximation can be made that:

(1) $B_{ii}\ |V_i|^2 \gg Q_i$.

(2) θ_i is closed to θ_k, $cos\theta_{ik} \approx 1$.

(3) $G_{ik}sin\theta_{ik} \ll B_{ik}$

Therefore, the power flow equation becomes:

$$\Delta P_i = -(B_{ik}|V_i||V_k|)\Delta\theta_k \quad (2.4.3.5)$$

$$\Delta Q_i = -(B_{ik}|V_i|)\ \Delta|V_k| \quad (2.4.3.6)$$

The final approximation is assuming it as a flat voltage profile, which is setting $|V_k| \approx 1$. Therefore, the decoupled load flow equations are:

$$\frac{\Delta P_i}{|V_i|} = -B_{ik}\Delta\theta_k \quad (2.4.3.7)$$

$$\frac{\Delta Q_i}{|V_i|} = -B_{ik}\Delta|V_k| \quad (2.4.3.8)$$

The transmission line model between bus i and bus k is shown below:

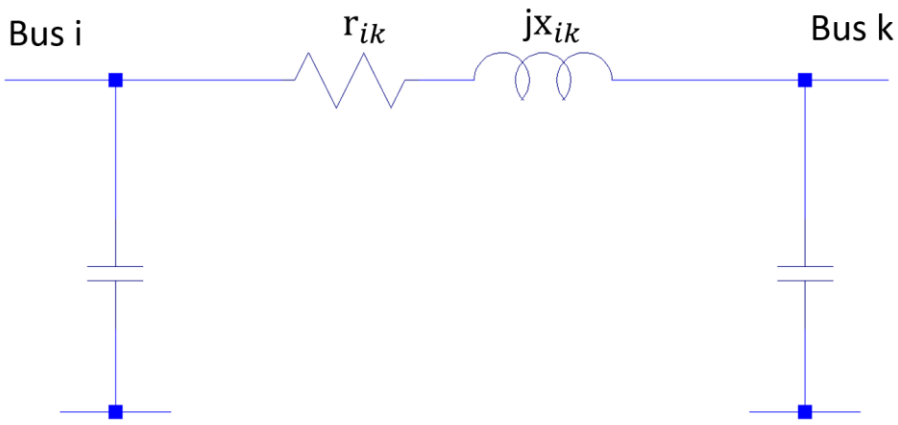

Figure 2. 2: Equivalent π model transmission line model between bus i and bus k

Where

r_{ik}=Resistance on the line between bus i and bus k.

x_{ik}=Reactance on the line between bus i and bus k.

y_{ci}, x_{ck}= Line charging admittance on the line between bus i and bus k.

When i is not equal to k, Y_{ik} is the off-diagonal element in Y_{bus}. The value of Y_{ik} is equal to the negative of admittance between bus i and bus k.

$$\begin{aligned} Y_{ik} &= G_{ik} + jB_{ik} \\ &= -y_{ik} \\ &= -(g_{ik} - jb_{ik}) \\ &= \frac{1}{r_{ik}+jx_{ik}} \\ &= \frac{r_{ik}}{{r_{ik}}^2+j{x_{ik}}^2} - j\frac{x_{ik}}{{r_{ik}}^2+j{x_{ik}}^2} \end{aligned} \qquad (2.4.3.9)$$

Therefore,

$$G_{ik} = -g_{ik} = \frac{r_{ik}}{{r_{ik}}^2+j{x_{ik}}^2} \qquad (2.4.3.10)$$

$$B_{ik} = b_{ik} = \frac{x_{ik}}{{r_{ik}}^2+j{x_{ik}}^2} \qquad (2.4.3.11)$$

For the DC power flow, a further assumption is ignoring the line resistance because the line reactance is much larger than the line resistance. Thus, B_{ik} becomes:

$$B_{ik} \approx \frac{1}{x_{ik}} \quad (2.4.3.12)$$

In addition, since the line resistance is so small that can be ignored, B matrix is an approximation of Y matrix. DC power flow is a simplified decoupled power flow that does not consider reactive power and voltage magnitude. Voltage magnitudes on all buses are assumed to be 1 per unit. The equation of DC power flow is:

$$P = B\,\theta \quad (2.4.3.13)$$

The real power flow on line l between bus i and k is:

$$f_l = \frac{1}{x_{ik}}\,(\theta_i - \theta_k) \quad (2.4.3.14)$$

DC power flow method provides a linear approximation relationship directly between power flow on line and bus voltage angle. In the later chapter, this approximation is used to estimate the spread of the impact of line outage contingency.

2.5 Contingency Analysis

Contingency analysis is the study of the outage of system elements: transmission lines, transformers, generators, and the evaluation of the impact on power flow redistribution and bus voltage change to the rest of system [28]. Contingency analysis is an important method for system operators to evaluate security and reliability of the system. It can be used to detect network weakness [29]. It can also help system operators predict the post-contingency condition and to make corrective action soon after contingencies to prevent serious trouble.

In the United States, for the reliability of power systems, the NERC(*n-1*) rule (North American Electric Reliability Corporation that sets the reliability standards for all electric system) states that no single outage will cause other components suffer from power or voltage limit violations, where *n-1* refers to one component outage in an *n* components system [30]. This work only considers *n-1* condition.

There are various methods for contingency analysis. This work uses DC load flow method to approximate post-contingency real power redistribution and AC load flow method to analyze how far the impact will spread.

2.6 IEEE 118 Bus System

IEEE 118 bus system describes an approximation of a part of Midwestern American Electric Power System. It includes 19 generators, 35 synchronous condensers, 186 branches, 9 transformers, and 91 loads [31]. In this work, IEEE 118 bus system is used to investigate the power redistribution after line contingency because it is large enough to observe the margin of the impact of the line outage. The detailed branch data, generation data, and load data is shown in Appendix.

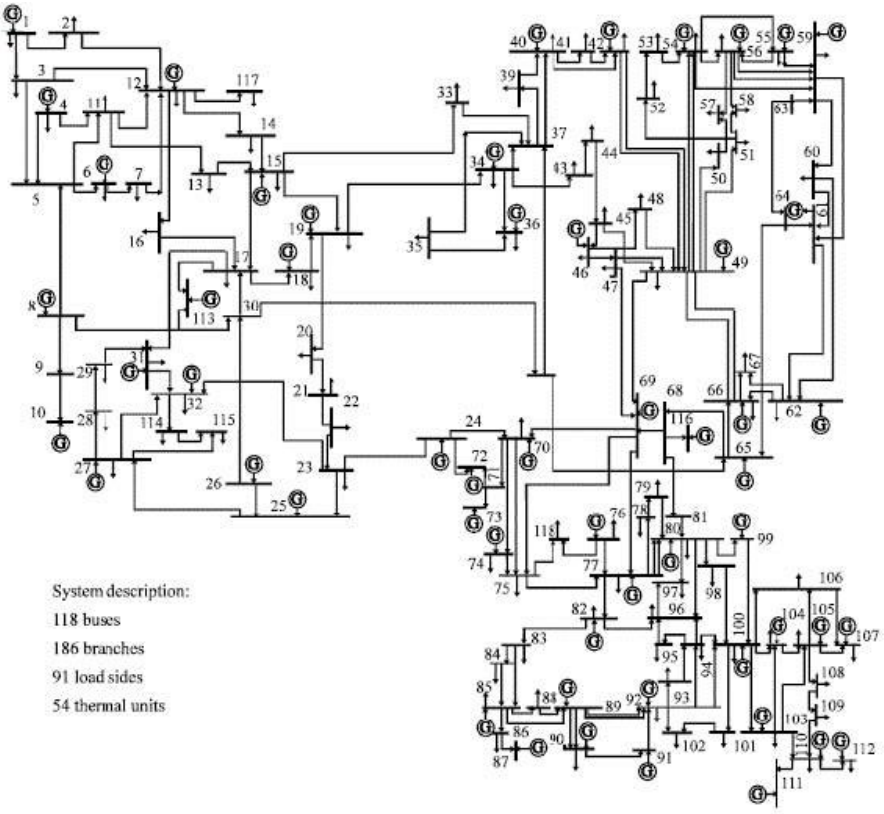

Figure 2. 3: IEEE 118 bus system diagram

2.7 Simulation Tool

This section describes the software used in this thesis. Besides the basic software like Microsoft Word and Excel, a toolbox inside Matlab called Matpower is the main tool used to do analysis.

MATPOWER is an open source programming package of MATLAB developed by Power System Engineering Research Center (PSERC) at Cornell. It performs steady-state power system analysis such as ac power flow, dc power flow, constrained power flows such as optimal power flow problems, security constrained economic dispatch, and even energy market studies. MATPOWER was intended as a simulation tool for researchers and educators, requiring running on licensing computer language MATLAB. In this study, the IEEE standard system models, power flow function, and optimal power flow function in MATPOWER are used.

Chapter 3: Active Power Flow Redistribution after Single Line Contingency

3.1 Introduction

In this chapter, the definition of Line Outage Distribution Factor (LODF) algorithm is presented to analyze the steady-state power flow redistribution in a network after a single line tripped. Due to Kirchoff voltage and current laws, the further the electric distance of a line from an outage is, the less effect that line will see. A line outage that happens should have a small or negligible effect on the active power change on distant lines. The definition of Thevenin electrical distance is introduced to quantify the electrical distance between lines. An exponential convergence tendency is observed between maximum possible LODF and electrical distance from outage line to other lines in the system. An exponential regression analysis is applied to obtain the equation between them.

IEEE 118 bus system is selected to implement LODF and Thevenin electrical distance algorithm in this chapter because it is large enough to observe the margin of the impact of line outage.

3.2 Line Outage Distribution Factor (LODF) Algorithm

3.2.1 Basic Theory

Generally, the power system network is operating in a steady-state condition where its total generations match total loads and power flow in the network remain unchanged. However, when a line outage happens, the steady-state of system is interrupted. In order to guarantee sufficient power flows from generators to loads, the rest lines in network have to carry the burden of the outage line and flow much power. Line Outage Distribution Factor (LODF) is a sensitivity factor which is often used to

analyze this situation. It approximates the steady-state active power flow variation on lines due to the outage of a single line in the network [18]. LODF is a percentage value which indicates the proportion between the change of active power flow on one line and the active power flow on the outage line before it tripped [32]. The advantage of this method is it can quickly estimate the steady-state impact of line outage to active power flow variation in the rest of system, and without solving a full ac Newton Rapson Iteration again. When both the system and the amount of line outage analyses are large, it will save much time and work. What is more, the results can be acquired directly from the system bus impedance matrix, Zbus. The change of load and generation condition will not affect its result.

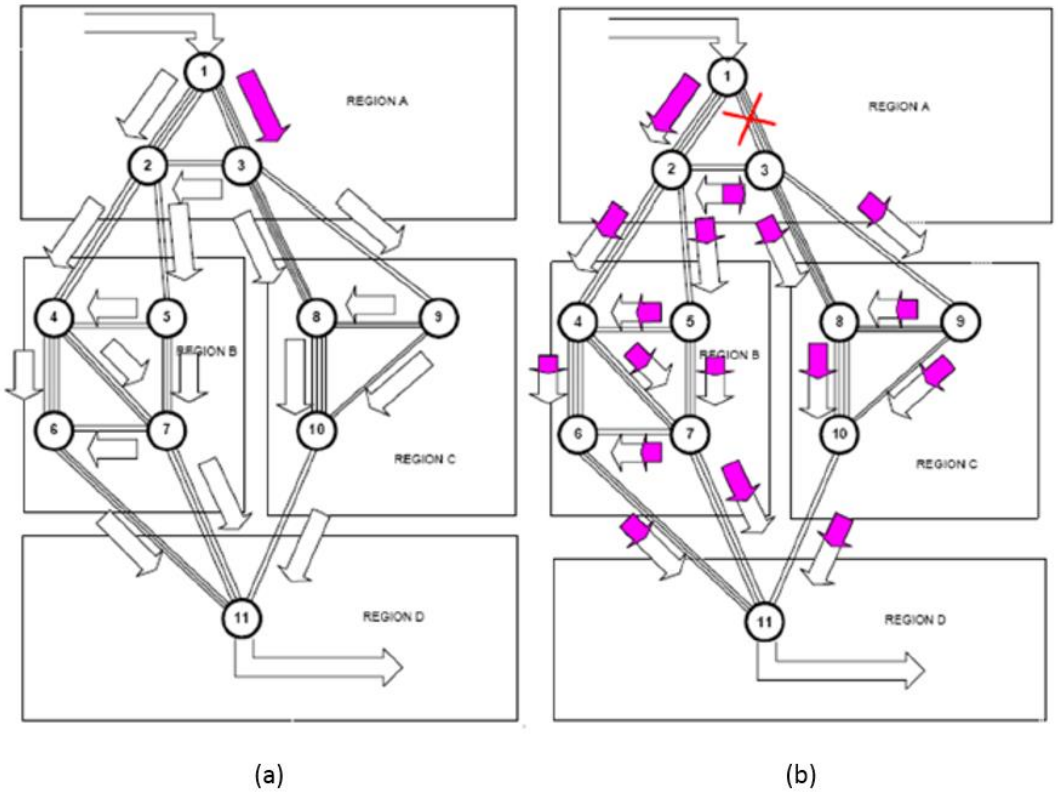

Figure 3. 1: (a) Power flow before line 1-3 outage (b) Power flow after line 1-3 outage [32]

Figure 3.1 presents power flow redistribution after a line outage happens. White arrows indicate the flow of power before the outage, while purple arrows in (b) show the variation of power flow on the rest of system due to the outage of line 1-3. If line k is tripped, the active power flow on l will become:

$$f_l = {f_l}^0 + LODF_{l,k}\ {f_k}^0 \qquad (3.2.1)$$

Where

$f_k^{\,0}$ = active power flow on line k before line l outage happens

$f_l^{\,0}$ = active power flow on line l before line l outage happens

$LODF_{l,k}$ = line outage distribution factor monitoring line l after an outage on line k. It always simplified as $d_{l,k}$ factor.

The derivation of LODF is based on the DC load flow model which is shown below.

In the previous chapter, DC load flow model gives the relationship between active power injections and voltage angle on bus as shown by:

$$\Delta \mathrm{P} = \mathrm{B}\Delta\theta \qquad (3.2.2)$$

Therefore,

$$\Delta\theta = \mathrm{B}^{-1}\Delta \mathrm{P} = \mathrm{X}\Delta \mathrm{P} \qquad (3.2.3)$$

The susceptance matrix B is an approximation of the Ybus matrix, and the reactance matrix X is an approximation of Zbus matrix.

The outage of line k between bus i and bus j in the system can be simulated by keeping line k in the network and adding two active power injections into bus i and bus j which can offset the power flow on the outage line. Therefore, line k is still connected in the network but it does not carry any power. The topology of the system is not changed, which means the reactance matrix X is not changed during calculation. Assuming the active power flow on line k before outage is P_{ij}, when two power injections $\Delta \mathrm{P}_i$ and $\Delta \mathrm{P}_j$ are added to bus i and bus j , the power flow on line k becomes $\widetilde{\mathrm{P}}_{ij}$.

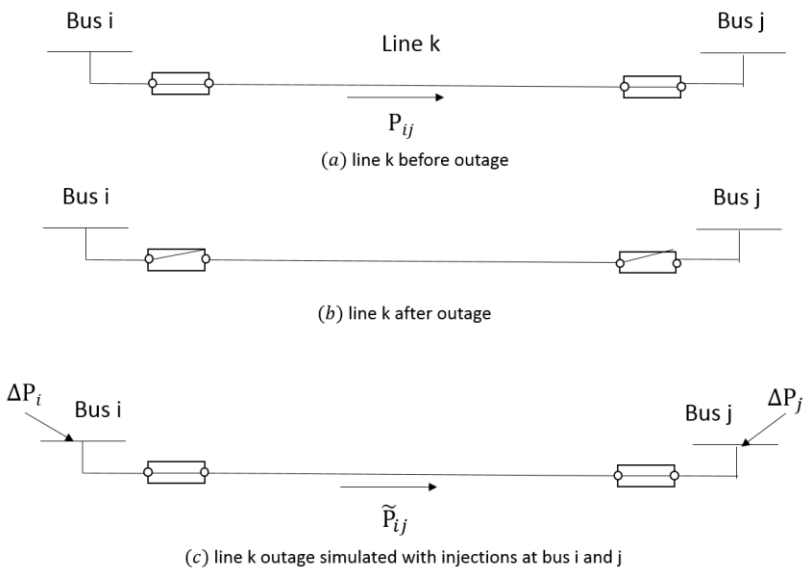

Figure 3. 2: The simulated model of the outage of line k.

The outage of line k can be simulated by:

$$\Delta P_i = \widetilde{P}_{ij} \tag{3.2.4}$$

$$\Delta P_j = -\widetilde{P}_{ij} \tag{3.2.5}$$

Let

$$\begin{aligned}\Delta P &= \left[0 \cdots \Delta P_i \cdots 0 \cdots \Delta P_j \cdots 0\right]^T \\ &= \left[0 \cdots \widetilde{P}_{ij} \cdots 0 \cdots -\widetilde{P}_{ij} \cdots 0\right]^T\end{aligned} \tag{3.2.6}$$

Therefore, the change of voltage angle on any bus m is:

$$\Delta\theta_m = \left(X_{mi} - X_{mj}\right)\Delta P_i \tag{3.2.7}$$

The changes of voltage angles on bus i and j are:

$$\begin{cases}\Delta\theta_i = X_{ii}\Delta P_i - X_{jj}\Delta P_j \\ \Delta\theta_j = X_{ij}\Delta P_i - X_{jj}\Delta P_j\end{cases} \tag{3.2.8}$$

The power flow on line k becomes:

$$\widetilde{P}_{ij} = \frac{1}{x_k}\left(\tilde{\theta}_i - \tilde{\theta}_i\right) \tag{3.2.9}$$

Where

$\tilde{\theta}_i = \theta_i + \Delta\theta_i$

$\tilde{\theta}_j = \theta_j + \Delta\theta_j$

x_k = reactance of the outage line k.

$$\therefore \widetilde{P}_{ij} = \frac{1}{x_k}\left(\theta_i - \theta_j\right) + \frac{1}{x_k}\left(\Delta\theta_i - \Delta\theta_j\right) \quad (3.2.10)$$

$$=> \widetilde{P}_{ij} = P_{ij} + \frac{1}{x_k}\left(X_{ii} + X_{jj} - 2X_{ij}\right)\Delta P_i \quad (3.2.11)$$

With $\widetilde{P}_{ij}$ is equal to ΔP_i,

$$\Delta P_i = P_{ij} + (X_{ii} + X_{jj} - 2X_{ij})\Delta P_i \quad (3.2.12)$$

$$\therefore \Delta P_i = \frac{1}{1 - \frac{1}{x_k}(X_{ii} + X_{jj} - 2X_{ij})} P_{ij} \quad (3.2.13)$$

$$\Delta\theta_m = \left(X_{mi} - X_{mj}\right)\Delta P_i \quad (3.2.14)$$

Substitute equation (3.2.13) into (3.2.14). When line k from bus i to bus j is tripped, the voltage angle variation on any bus m is:

$$\Delta\theta_m = \frac{x_k * P_{ij}}{x_k - (X_{ii} + X_{jj} - 2X_{ij})} (X_{mi} - X_{mj}) \quad (3.2.15)$$

As mentioned above, $LODF_{l,k}$ gives the impact on real power flow on line l when line k is tripped.

$$LODF_{l,k} = d_{l,k} = \frac{\Delta f_l}{P_{ij}} \quad (3.2.16)$$

Where Δf_l is the active power flow change on any line l in the system.

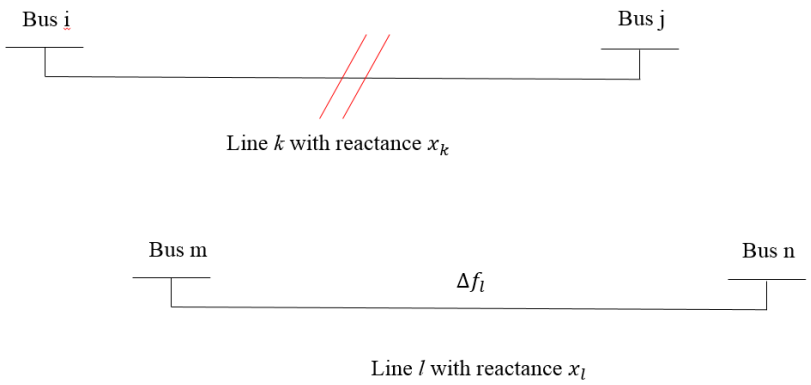

Figure 3. 3: Illustration of the outage of line k.

If line l locates between bus m and bus n, then

$$\Delta f_l = \frac{1}{x_l}(\Delta\theta_m - \Delta\theta_n) \qquad (3.2.17)$$

Where x_l is the reactance on line l.

Replace equation (3.2.7) into equation (3.2.17). As a result of the outage of line k (between bus i and bus j), the LODF of line l (between bus m and bus n) is:

$$\begin{aligned} d_{l,k} &= \frac{\Delta f_l}{\mathrm{P}_{ij}} \\ &= \frac{1}{x_l * \mathrm{P}_{ij}}(\Delta\theta_m - \Delta\theta_n) \\ &= \frac{1}{x_l}\left(\frac{x_k*(\mathrm{X}_{mi}-\mathrm{X}_{mj})-x_k*(\mathrm{X}_{ni}-\mathrm{X}_{nj})}{x_k-(\mathrm{X}_{ii}+\mathrm{X}_{jj}-2\mathrm{X}_{ij})}\right) \\ &= \frac{x_k}{x_l}\left(\frac{\mathrm{X}_{mi}-\mathrm{X}_{mj}-\mathrm{X}_{ni}+\mathrm{X}_{nj}}{x_k-(\mathrm{X}_{ii}+\mathrm{X}_{jj}-2\mathrm{X}_{ij})}\right) \end{aligned} \qquad (3.2.18)$$

3.2.2 Implementation of Line Outage Distribution Factor Algorithm on IEEE 118 bus system

The derivation of LODF has been shown in the previous section while in this part, it will be implemented in the IEEE 118 bus system. The system parameters of it are shown in Appendix. The testing results will be utilized in the following analysis of how the impact of line outage will expand.

Matpower, introduced in Chapter 2.7, is where the implementation of the LODF algorithm being processed. The first step is calculating the Zbus matrix, which is approximated as reactance matrix X according to the branch data in the Appendix and the method in chapter 2.2. The X matrix is a 118×118 full matrix. Then, the next step is to run a full AC load flow one time to obtain the normal operating condition of network, and the LODF can be calculated by equation (3.2.18) with Zbus data and branch data. Multiplying the result by the original active power flow on the outage line will be the predicted power flow variation on all lines. For a single line outage case, 186 of factors can be obtained, which demonstrates the ratio between active power flow variations on all the lines in the system and active power flow on the outage line. Testing outage of line 8-5 as an example. The original active power flow on it is 388.5 MW which is a heavy-loaded line in the left part of the IEEE 118 bus system. When the line between bus 8 and bus 5 is tripped, the equation of LODF of line l between buss m and n turns out to be:

$$d_{l,8-5} = \frac{x_{8-5}}{x_l}\left(\frac{\mathrm{X}_{m8}-\mathrm{X}_{m5}-\mathrm{X}_{n8}+\mathrm{X}_{n5}}{x_{8-5}-(\mathrm{X}_{88}+\mathrm{X}_{55}-2\mathrm{X}_{85})}\right) \qquad (3.2.19)$$

The results of LODF when line 8-5 is tripped with branch index l varying from 1 to 186 is:

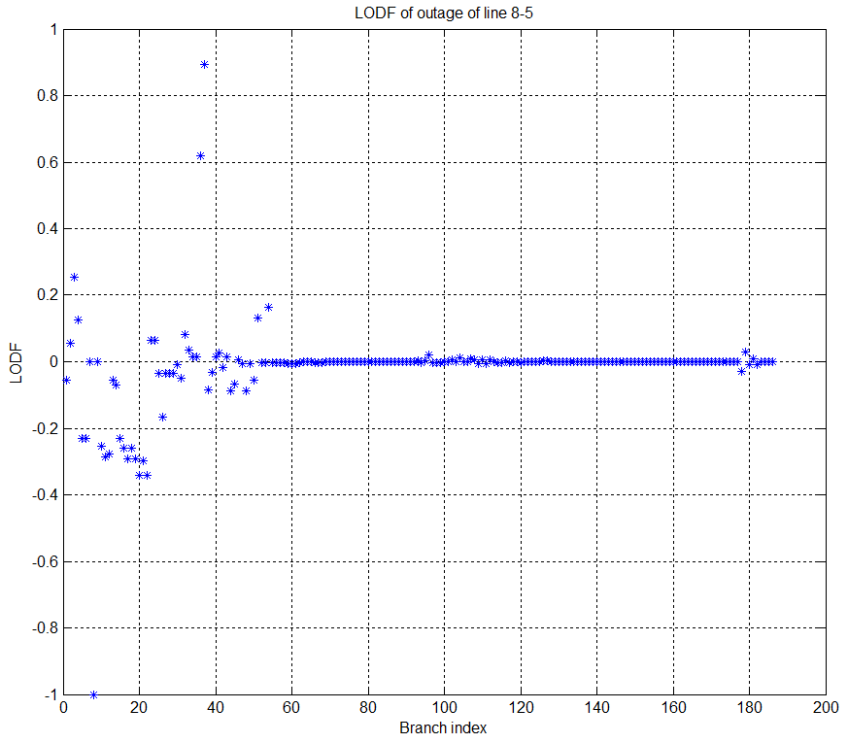

Figure 3. 4: LODF results when line 8-5 is tripped

To predict active power change on all lines with LODF results when line 8-5 is tripped, multiply LODF values by the original active power on line 8-5 which is obtained from the normal operating condition according to equation (3.2.18).

$$\Delta f_l = \mathrm{d}_{l,8-5} * \mathrm{P}_{85} \qquad (3.2.20)$$

Where

P_{85} = Active power flow on line 8-5 before the contingency in MW, which is 388.5

Δf_l = Active power flow variation on line *l* in the system

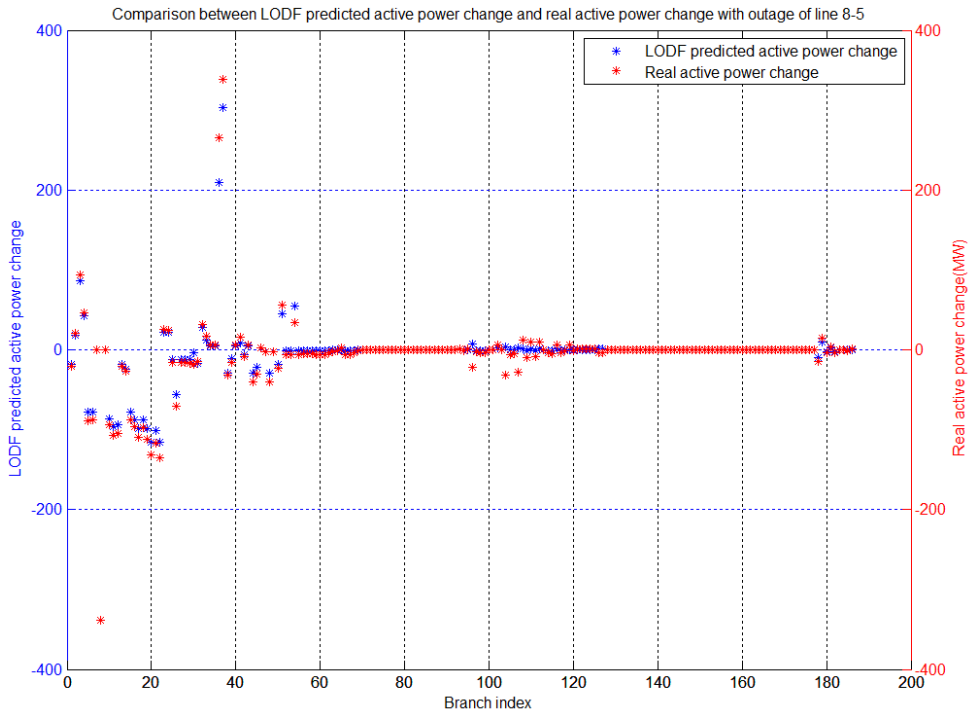

Figure 3. 5: Comparison between LODF predicted active power variations and real active power variations when line 8-5 tripped

As shown in the figure, the blue dots represent the LODF predicted active power flow variation on all lines in MW and the red dots are the real active power flow variation. For this case, most of the 186 predicted data points greatly match the real data except for branch 36 and 37, whose errors are 24.2% and 48.1%. The errors of all other 184 data are below 5%. Therefore, the accuracy of LODF prediction is 98.9%. The result of LODF data gives a decent prediction of active power change on all lines when line 8-5 is tripped.

After that, the LODF algorithm is implemented to all possible outage cases in the IEEE 118 bus system. Assume the generation and load conditions of system remains unchanged before and after line is tripped. Therefore, the outage cases which may make system becomes islanded are not considered in this work. There are 176 possible line outage cases overall and all of them are tested by LODF algorithm. The result is a 176×186 full matrix. With 176×186 LODF predicted data points, there are only 168 data points have error larger than 5%. Therefore, the accuracy of LODF prediction is $\frac{176\times186-168}{176\times186}\times 100\%$, which is 99.49%. Thus, a conclusion can be made that LODF can give a superior estimation of the steady-state active power variations for all possible line

outage cases in the IEEE 118 bus system. The LODE predicted power flow variations result will be applied to analyze the spread of steady-state effect of line outage in the later sections.

3.3 Lines location as a Function of Thevenin Impedance from an Event Location

Due to Kirchoff voltage and current laws, the further the electric distance of a line from an outage is, the less effect that line will see. A line outage that happens should have small or negligible effect on the active power change on distant lines.

To quantify the location of transmission lines, Thevenin electrical distance between transmission lines is introduced as follows.

The concept of electrical distance was first proposed by Lagonotte P in [24]. It is an electrical quantity which is used to describe electrical coupling between buses. Until now, several valuable methods have been developed to express electrical distance but people have not come to a consensus yet. This work uses the Thevenin impedance method to describe electrical distance between buses (the detailed derivation was introduced in Chapter 2.3). The Thevenin impedance between bus j and bus k is:

$$Z_{th,jk} = \frac{\mathrm{V}_{oc,kj}}{\mathrm{I}_{sc,kj}} = X_{jj} + X_{kk} - 2X_{jk} \qquad (3.3.1)$$

Where

X_{jk}= transfer reactance between bus j and bus k

X_{jj}= driving reactance of bus k

It implies that the closer the values of transfer reactance (X_{jk}) and driving reactance (X_{jj} and X_{kk}) are, the lower mutual electrical distance is and the stronger the coupling between bus j and bus k is.

Equation (3.3.1) shows the electrical distance between two single nodes. Due to electricity following the path of least resistance, an assumption can be made that electrical distance between any line l and the outage line k is approximated by the

shortest electrical distance of the buses connected by the line *l* and buses connected by the line *k*. The illustrative example is shown below:

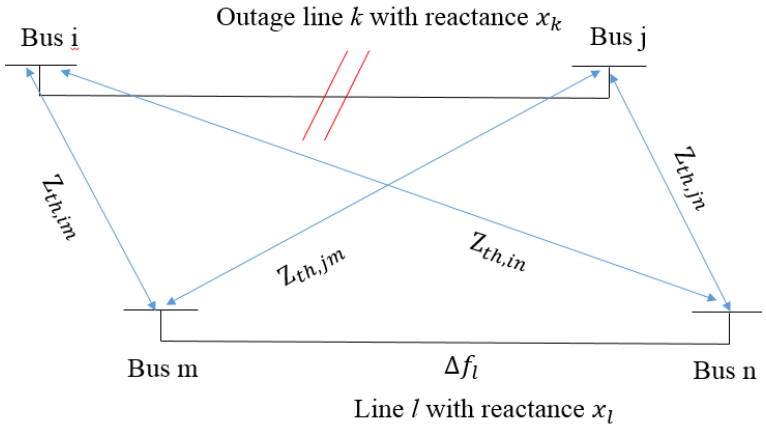

Figure 3. 6: Illustration of electrical distance between the outage line k and line l

The equation of Thevenin equivalent electrical distance from the outage line k to any single line l in the system is:

$$\mathrm{Z}_{th,k-l} = \min(\mathrm{Z}_{th,im}, \mathrm{Z}_{th,in}, \mathrm{Z}_{th,jm}, \mathrm{Z}_{th,jn}) \qquad (3.3.2)$$

The unit of Thevenin equivalent electrical distance is per unit.

The assumption can be made that the impact of contingency in the system, such as line outage, will be negatively related with Thevenin equivalent electrical distance between lines. Lines with an electric distance large enough will not be impacted by the contingency.

3.4 Analysis of impact of single line outage in IEEE 118 bus system

When a line outage happens in system, equation (3.2.15) demonstrates how the voltage angle variation on any bus *m* due to an outage of the line from bus *i* to bus *j*:

$$\Delta\theta_m = \frac{x_k * \mathrm{P}_{ij}}{x_k - (\mathrm{X}_{ii} + \mathrm{X}_{jj} - 2\mathrm{X}_{ij})} (\mathrm{X}_{im} - \mathrm{X}_{jm}) \qquad (3.4.1)$$

The algorithm was tested on the outage of line 8-5, as shown in Figure 3.7, which is a heavy-loaded line in the left part of the system with a 338.5 MW flow on it.

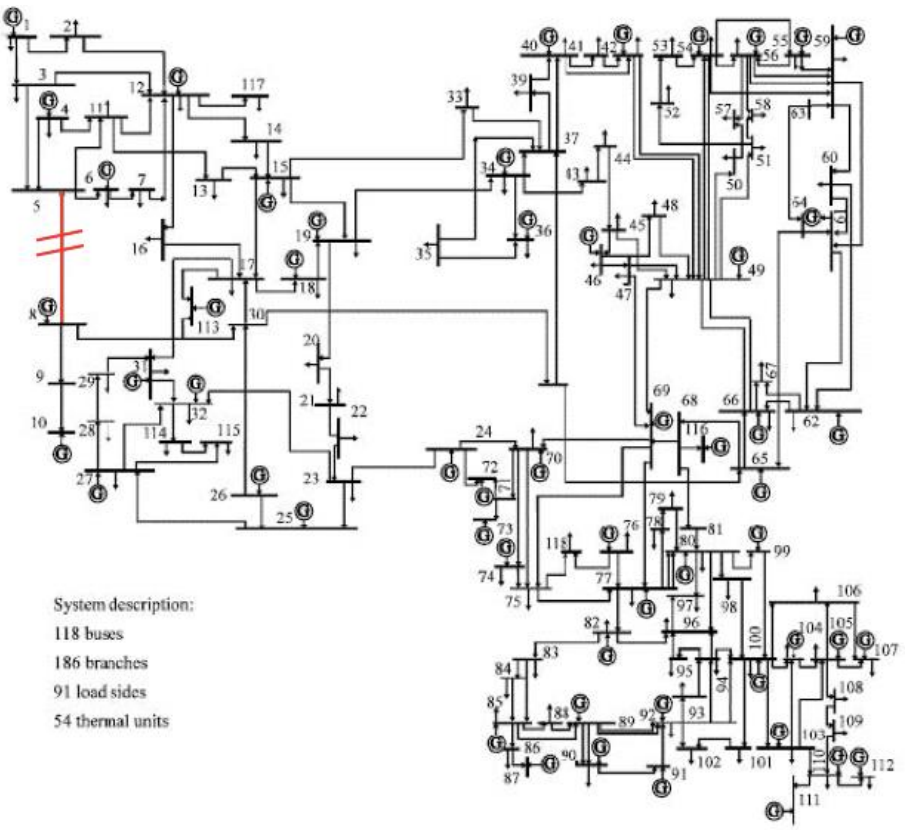

Figure 3. 7: IEEE 118 bus system with line 8-5 outage

Let

$$K = \frac{x_{ij} * P_{ij}}{x_{ij} - (X_{jj} + X_{ii} - 2X_{ij})} \tag{3.4.2}$$

Equation (3.4.1) can be simplified to:

$$\Delta\theta_m = K\,(X_{jm} - X_{im}) \tag{3.4.3}$$

Taking parameters of line 8-5 outage into equation 3.4.1, the voltage angle variation on any bus *m* becomes:

$$\Delta\theta_m = \frac{x_{8-5} * P_{85}}{x_{8-5} - (X_{55} + X_{88} - 2X_{85})}\,(X_{5m} - X_{8m}) \tag{3.4.4}$$

Due to line resistance, elements in impedance matrix, and original active power flow on the outage line are fixed value, the value of K is constant for this line outage case.

Therefore, the change of voltage angle on any bus m is linearly proportional to the difference between transfer reactances X_{5m} and X_{8m}. This is because the linear

relationship between active power flow and voltage angle in the DC model. The following figure is the plot of X_{m5} and X_{8m} for m varying from 1 to 118.

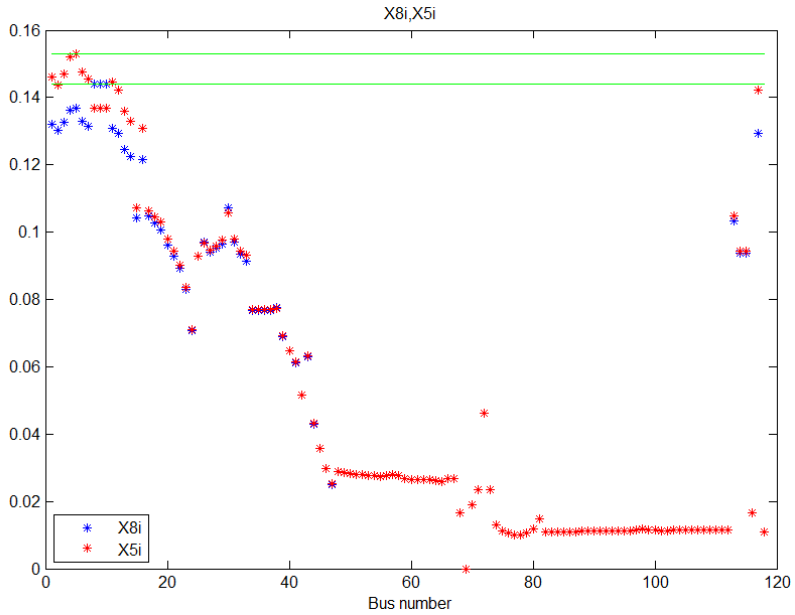

Figure 3. 8: Plot of X_{8m} and X_{5m}

As shown in the figure, those buses with larger values of X_{8m} and X_{5m} have large differences between X_{8m} and X_{5m}, which means the voltage angle variations on these buses are large. For those buses with smaller values of X_{8m} and X_{5m}, the differences between them are very small. Therefore, the voltage angle variations on these buses are also small or even negligible. Therefore, the outage of line 8-5 can only impact the voltage angle variations on those buses with large values of X_{8m} and X_{5m}.

Dividing all 118 buses into three areas according to the values of X_{8m} and X_{5m} varies from large to small, the result is shown below.

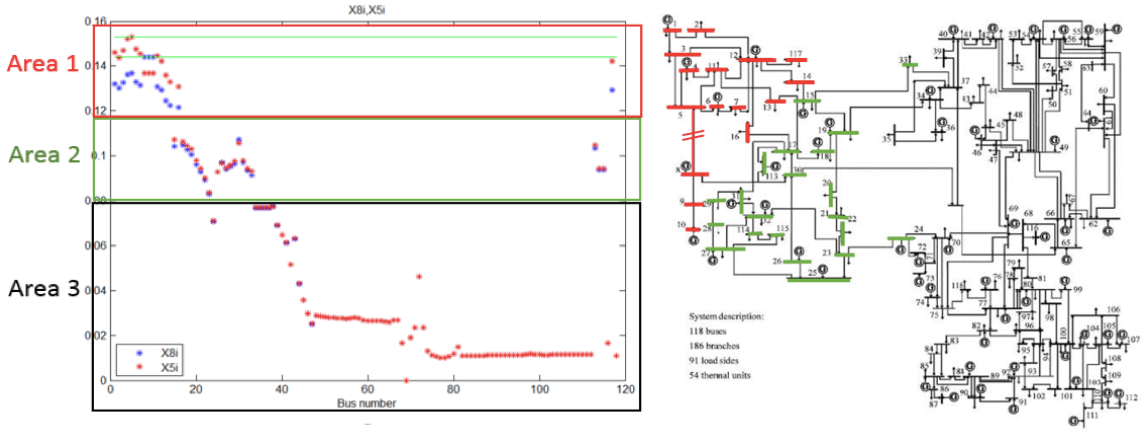

Figure 3. 9: (a) X_{8m} and X_{5m} (b) IEEE 118 bus system with line 8-5 outage

As demonstrated in Figure 3.9 (a), buses in area 1 have the largest values of X_{8m} and X_{5m}. The differences between X_{8m} and X_{5m} are also the largest. In area 2, the X_{8m} and X_{5m} values of these buses become smaller, and the differences between X_{8m} and X_{5m} are also smaller. The rest of the buses are in area 3, which have the smallest values of X_{8m} and X_{5m}. Buses in this area have almost the same values of X_{8m} and X_{5m}. This shows that voltage angles on these buses are almost unchanged, which means these buses are free from the impact of the line 8-5 outage. In Figure 3.9 (b), buses in area 1, 2, 3 are respectively marked in red, green, and black. As can be seen in this figure, all of the buses in area 1 are neighboring buses of the outage line. The voltage angles on buses in this area have the largest change. Buses in area 2 are further from the outage line, whose voltage angle changes are less affected than buses in area 1. Buses in area 3 are the furthest buses from line 8-5. They are almost free from the impact of an outage of line 8-5. A trend can be seen that the spread of the impact of the line 8-5 outage on voltage angle variations is negatively related with distance. The impact of line 8-5 outage on voltage angle variations can be regarded as an outward radiation starting from line 8-5. The illustration is shown below in Figure 3.10.

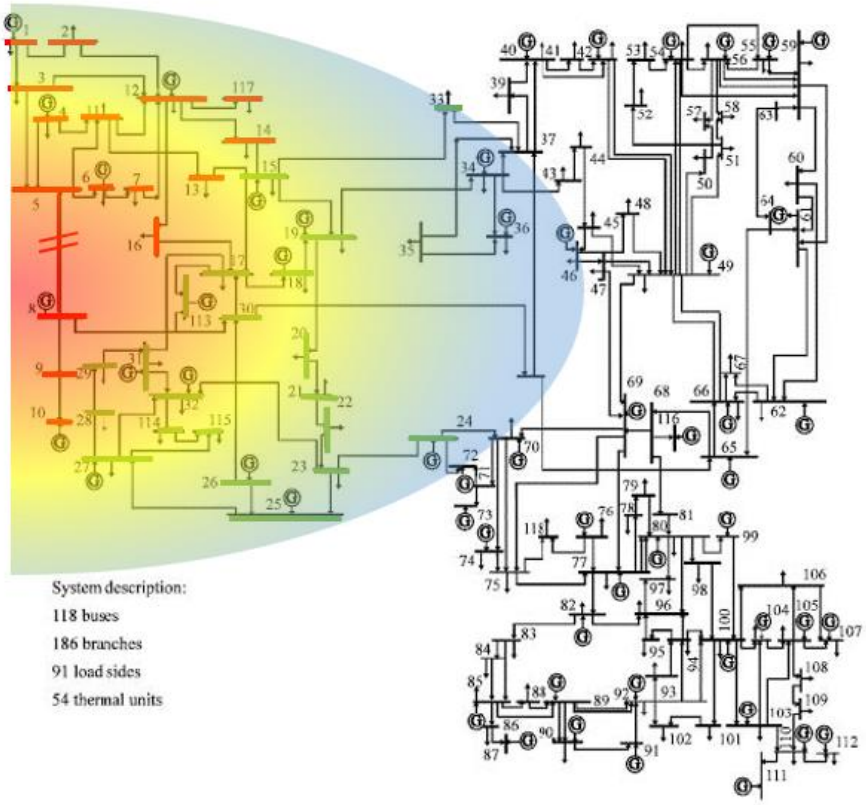

Figure 3. 10: Radiate shape impact of line 8-5 outage on voltage angle variations in IEEE 118 bus system

As mentioned in Chapter 3.3 that the closer distance between values of transfer reactance (X_{jk}) and driving reactance (X_{jj} and X_{kk}) is, the closer mutual electrical distance and the stronger the coupling between bus j and bus k is. This theory can be verified by the simulation results of a line 8-5 outage case in the IEEE 118 bus system. As shown in Figure 3.9 (a), buses in area 1 have the largest values of X_{8m} and X_{5m}, while they have the smallest differences between values of transfer reactance (X_{8m} and X_{5m}) and driving reactance (X_{88} and X_{55}) which are the two green lines on the top of the Figure 3.4). Also, buses in area 1 are the electrically adjacent buses of the outage line 8-5. Similarly, buses in area 3 have the largest difference between values of transfer reactance and driving reactance and they are electrical furthest buses. Therefore, according to the equation (3.3.1) which gives the electrical distance between bus *i* and bus *j*, an assumption can be made that electrical distance between a line and a bus j may be approximated by the shortest electrical distance of the buses connected by the line and

any bus m. This is due to the electricity following the path of least resistance. The electrical distance between outage line 8-5 and any bus m can be obtained as:

$$Z_{th,m-85} = \min(Z_{th,m8}, Z_{th,m5}) \tag{3.4.5}$$

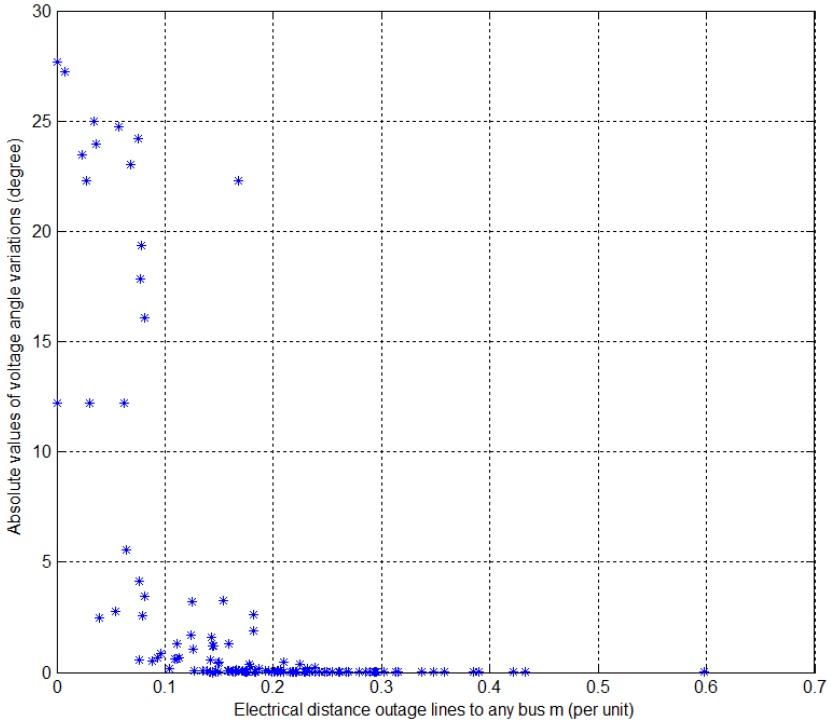

Figure 3. 11: Absolute values of voltage angle variations (degree) vs. Electrical distances from the outage line to any bus m

It can be seen in Figure 3.11 that the absolute values of voltage angle variations converge as the electrical distance increases, which illustrates that voltage angle variation is inversely proportional to the electrical distance between bus *m* and outage line. For the buses with the electrical distance larger than 0.181 per unit, the voltage angles on them will not be affected by the outage.

After the changes of voltage angle on all buses has been analyzed, according to the DC load flow equation (2.4.3.14), the change of power flow on any line *l* in the system between buses *m* and *n* can be calculated as

$$\Delta f_l = \frac{1}{x_l}(\Delta\theta_m - \Delta\theta_n) \tag{3.4.6}$$

Where x_l is the reactance of line *l*.

As shown in the equation, when a line outage happens, the power flow variation on any line *l* is determined by two parts:

(a) The value of line reactance x_l.

(b) The difference between changes of voltage angle of buses *m* and *n*.

Line reactance is a physical parameter of transmission lines that varies for different lines, but is within a specific positive number range. However, the difference between changes of voltage angle of connected buses can vary from negative to positive values in a larger range, which has a greater impact on the value of Δf_l.

As discussed above, the voltage angle variations are negatively related with electrical distance. For a single line outage case, the impact on voltage angle change on buses will drop to zero outside of a certain electrical distance. Therefore, there will be three possible situations for active power flow variation on line *l* between bus *m* and bus *n*.

(a) If both bus *m* and bus *n* are electrically close buses to the outage line, the magnitude of $\Delta\theta_m$ and $\Delta\theta_n$ are both large. It is possible that Δf_l is large when $\Delta\theta_m$ and $\Delta\theta_n$ have different signs or have the same sign but with different magnitudes. It is also possible that Δf_l is small when $\Delta\theta_m$ and $\Delta\theta_n$ have the same sign and similar magnitude.

(b) If bus *m* is electrically close, and bus *n* is electrically distant, $\Delta\theta_m$ is large and $\Delta\theta_n$ is small Δf_l is large.

(c) If both bus *m* and bus *n* are electrically distant buses, Δf_l is negligible.

In conclusion, the lines connected to at least one electrically close bus to the tripped line, will be possible to have a large change of real power flow on it. As the electrical distance from the outage line increases, the maximum possible active power variations on lines will decrease due to the decrease of the maximum possible bus voltage angle variations. The lines connected to two electrically distant buses will not be affected by the line outage.

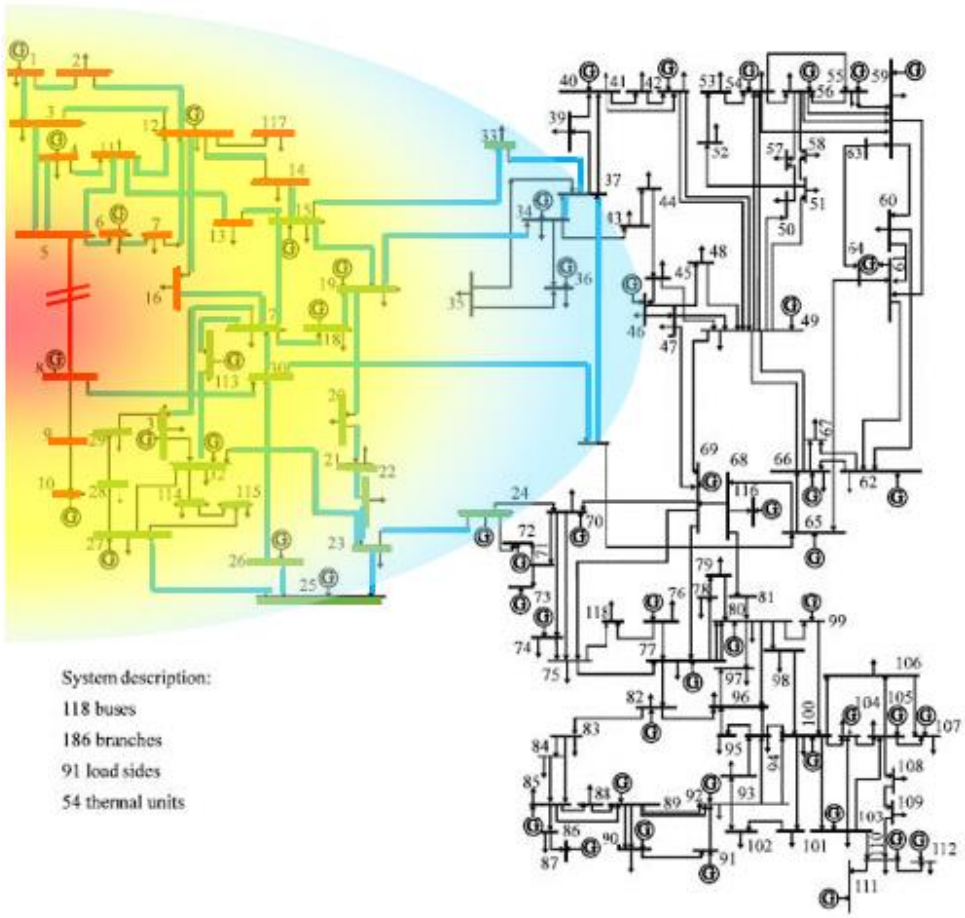

Figure 3. 12: Radiate shape impact of line 8-5 outage on voltage angle and power flow variations in IEEE 118 bus system

All the marked blue lines in Figure 3.12 are lines with a change of power flow larger than 10 MW in the network. Compared with 338.5 MW on line 8-5 before the outage happens, any line with a change of power flow under 10 MW can be regarded as the impact of outage is negligible. As can be seen in the figure, all the blue lines are covered by the arch radiation area, which are all connected to the electrically close buses to outage line. In addition, on the lower left corner of the radiation area, several lines in black are connected to electrically close buses to the outage line but have negligible power change on them. This phenomenon verifies the previous statement that Δf_l will be small when both bus *m* and bus *n* are electrically close buses to the outage line but $\Delta\theta_m$ and $\Delta\theta_n$ have the same signs and same magnitude.

Therefore, it can be concluded that the active power change on electrically close lines can be large or small. As electrical distance increases, the maximum possible power variation decreases. As electrical distance increases to a certain value, the lines beyond this limit are free from the impact of the outage line.

Calculating the electrical distances from line 8-5 to each line in the system by equation (3.3.2) and mapping them to corresponding LODF predicted power flow variations calculated in Chapter 3.2, the result is shown as follows.

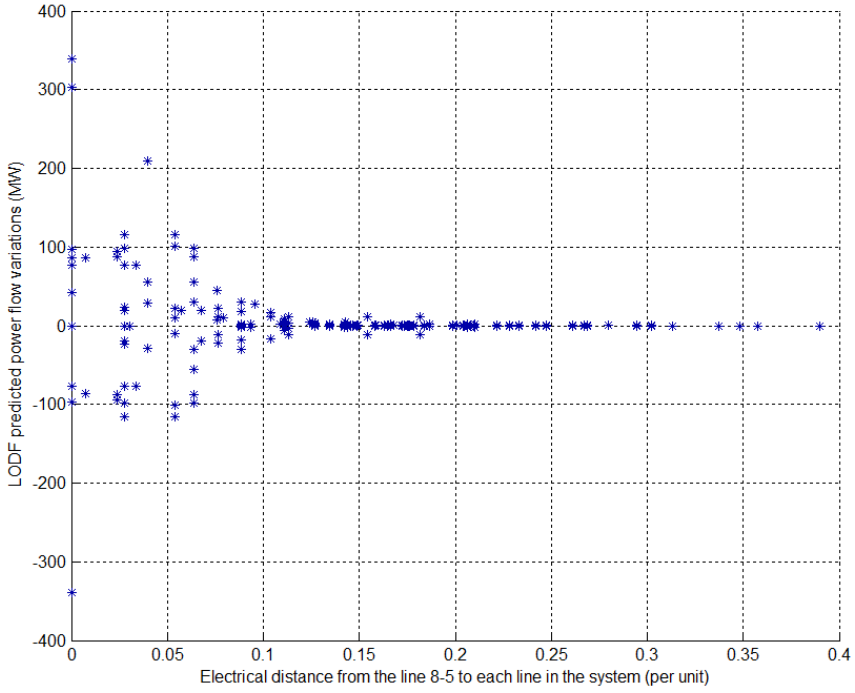

Figure 3. 13: LODF predicted power flow variation of each line vs. Electrical distance from line 8-5 to each line in the system

A tendency of convergence can be seen in the figure. As discussed above, active power flow variation on the electrically close lines can be large or small. As electrical distance grows, the maximum possible change will keep dropping until it reaches zero.

The result of taking the absolute value of LODF predicted power flow variations to observe only the magnitude of the change of active power on transmission lines is shown in Figure 3.14.

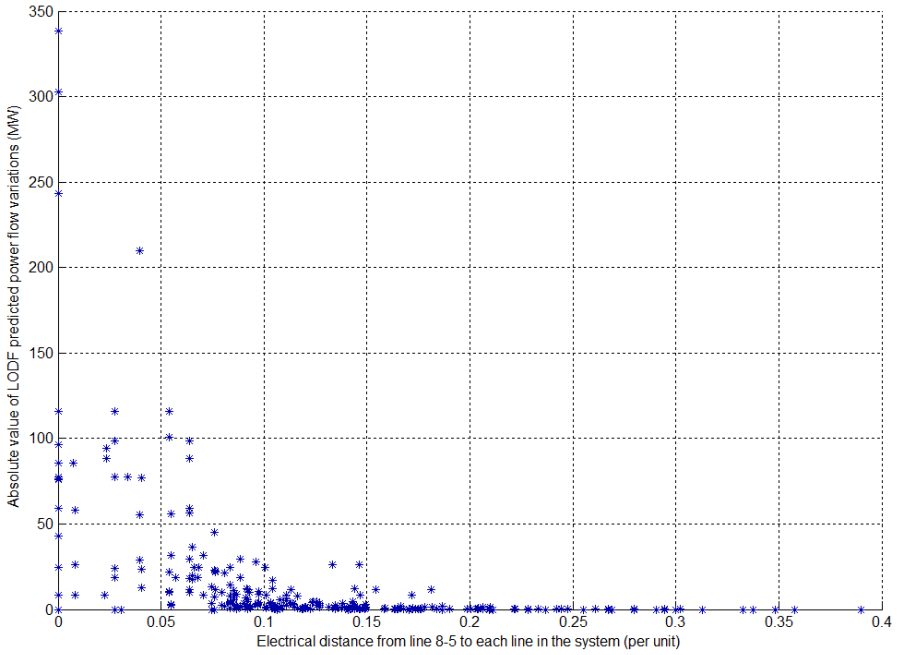

Figure 3. 14: The absolute value of LODF predicted power flow variation of each line vs. Electrical distance from line 8-5 to each line in the system

As can be seen in the figure, the boundary of the absolute value of LODF data drops quickly to zero in the electrically close area and slows down when the distance becomes larger. Assuming the lines are free from the contingency if the power variations on them are smaller than 10 MW. The lines with electrical distances larger than 0.181 per unit are not affected by the outage of line 8-5. It can be seen the boundary of the absolute value of the LODF data is non-linearly converging to zero.

The same analysis was conducted for an outage of the line 38-37, which is a heavy-loaded line in the middle part of the system with 243 MW power on it. The result is shown in Figure 3.15.

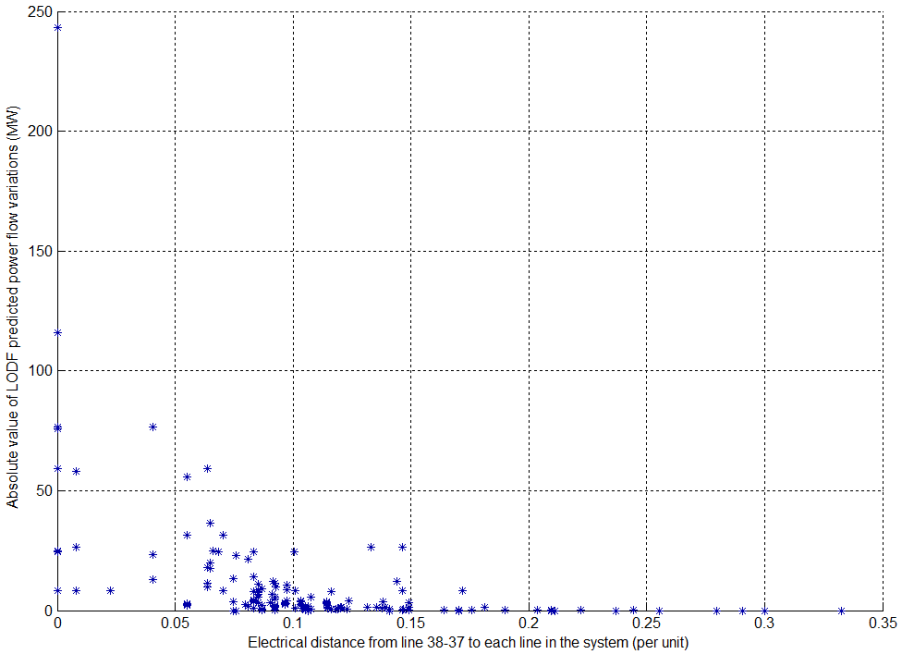

Figure 3. 15: Absolute value of LODF predicted power flow variation of each line vs Electrical distance from line 38-37 to each line in the system

Similarly, a non-linear trend of convergence shows up again between the boundary of the absolute values of the LODF data and electrical distances. 0.147 per unit is the furthest electrical distance the impact of contingency can reach (assuming the lines are free from the contingency if the power variations on them are smaller than 10 MW).

This analysis was repeated for all 176 line contingency cases. The result can be seen below:

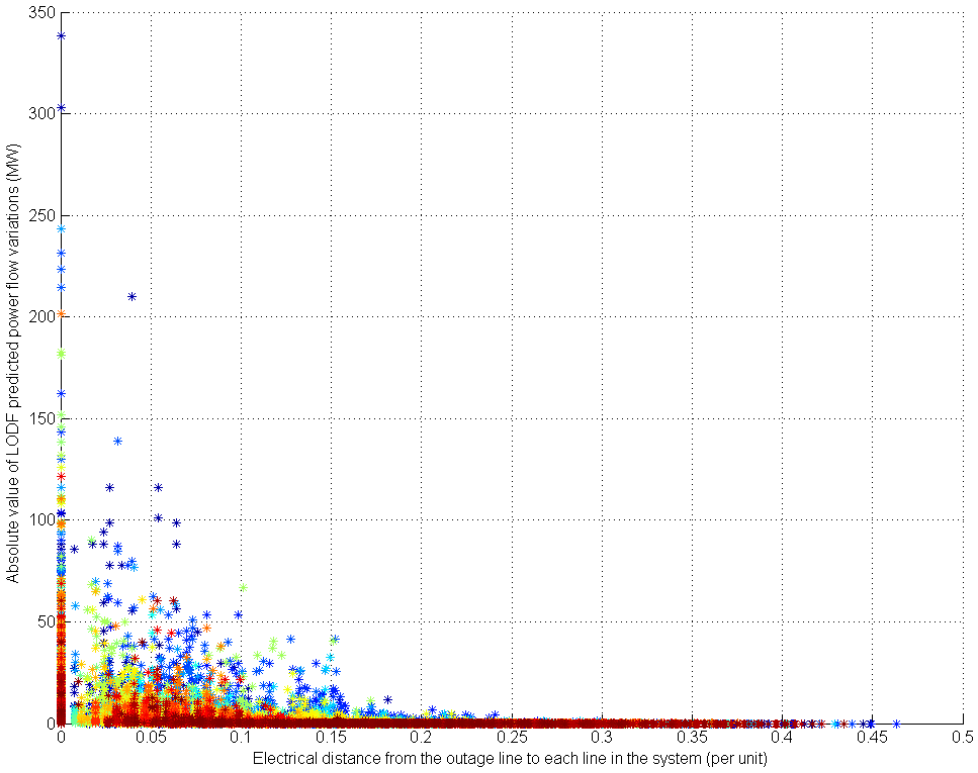

Figure 3. 16: Absolute value of LODF predicted power flow variations of each line vs. Electrical distances between lines to outage lines for all possible 176 line outage cases

In this figure, each color indicates a single line outage case in the IEEE 118 bus system. A non-linear convergence tendency can be seen for all line outage cases. For all line outage cases, the lines with electrical distances larger than around 0.181 per unit have negligible impact of the line outage (assuming the lines are free from the contingency if the power variations on them are smaller than 10 MW). A statistical method to predict the spread of the impact of a line outage in the IEEE 118 bus system will be discussed in next section.

3.5 Exponential Regression Method to Predict Impact of Single Line Outage on Active Power Flow Redistribution

In the previous section, when a single line outage happens in the IEEE 118 bus system, a non-linear convergence tendency has been found between the boundary of the absolute value of LODF predicted power flow variations of each line and electrical distances between lines. Additionally, for each of the line outage case, as the electrical

distance increases to a certain value, lines beyond this limit are free from the impact of the line outage contingency. The maximum limit is observed as 0.181 as shown in the previous section. This phenomenon verifies the statement proposed in Chapter 3.3 that the maximum possible active power variations on lines are negatively related with the Thevenin equivalent electrical distances. Therefore, with the knowledge of this tendency, the question becomes how to quantify and formulate the convergence of the boundary.

Non-linear regression method is a reasonable way to solve the relationship between the boundaries of absolute value of LODF predicted power flow variations and electrical distances. After the testing of several non-linear models, such as logarithmic, exponential, and power regression model, the exponential regression model was found to best fit the relationship between the boundary of the absolute value of LODF data and electrical distances from the outage line to other lines.

When the i^{th} line outage happens in the system, each line in the system is assigned with an absolute LODF predicted power flow variation value and an electrical distance, A scatter plot is formed by the 186 data points (as show in Figure 3.14 and Figure 3.15). From observation, 11 to 14 representative boundary points can greatly represent the boundary condition of the scatter plots of a line outage case. In line 8-5 outage case, 13 representative boundary points are selected to form the dataset for the exponential regression analysis. The absolute LODF predicted power flow variations and electrical distances for these selected data points are represented as $[|\mathrm{LODF}|]_i$ and $[\mathrm{x}]_i$. $[|\mathrm{LODF}|]_i$ are dependent variables and $[\mathrm{x}]_i$ are independent variables. Therefore, the exponential regression model is:

$$[|\mathrm{LODF}|]_i = a_i * \exp(\mathrm{b}_i * [\mathrm{x}]_i) \text{ for i} = 1,2,\dots,176 \qquad (3.5.1)$$

Where a_i and b_i are the exponential regression model coefficients. 176 is the total number of possible line outage cases in the IEEE 118 bus system. With the selected datasets, coefficients a_i and b_i can be determined to best approximate the relationship between the boundary of the absolute value of LODF predicted power flow variations and electrical distances.

The exponential regression model is implemented to the IEEE 118 bus system. When line 8-5 is tripped, the relationship between the LODF data and electrical distances of all 186 lines is shown in Figure 3.16. Taking outage of line 8-5 as an example for exponential regression analysis, the index of line 8-5 outage is i=7. Column vector $[|\text{LODF}|]_7$ contains absolute values of LODF predicted power flow variations of the selected boundary points, and $[\text{x}]_7$ contains absolute values of electrical distances of them. The selected boundary points are shown as red points in the figure below.

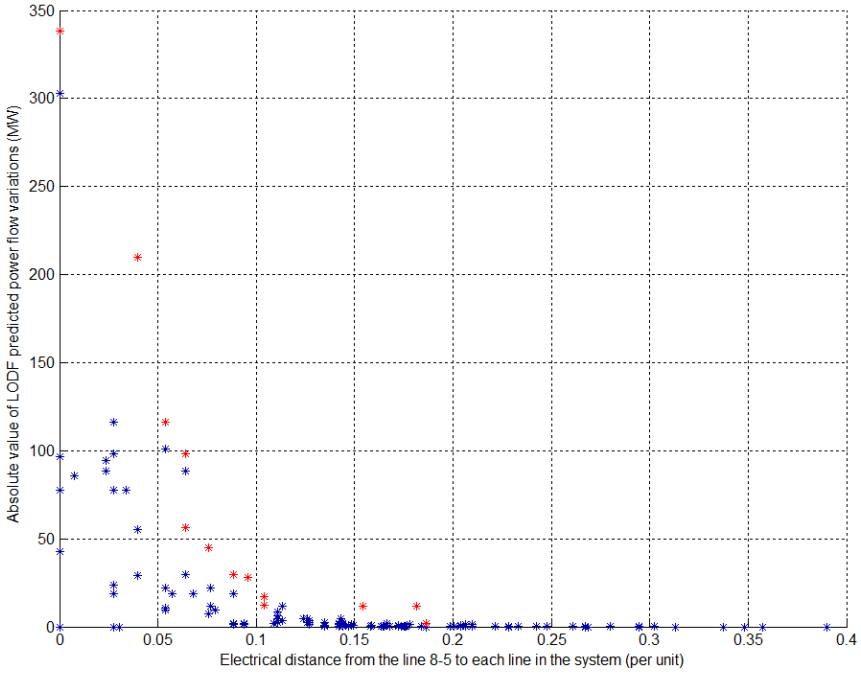

Figure 3. 17: Absolute value of LODF predicted power flow variation of each line vs. Electrical distance from line 8-5 to each line in the system

The exponential regression model of line 8-5 outage case is:

$$[|\text{LODF}|]_7 = a_7 * \exp(\text{b}_7 * [\text{x}]_7) \qquad (3.5.2)$$

Where

$$\begin{bmatrix} 338.5 \\ 209.9 \\ 116.1 \\ 98.5 \\ 56.2 \\ 44.9 \\ 29.6 \\ 27.8 \\ 17.0 \\ 12.0 \\ 11.9 \\ 11.9 \\ 1.7 \end{bmatrix} = a_7 * \exp(\mathrm{b}_7 * \begin{bmatrix} 0 \\ 0.0395 \\ 0.0538 \\ 0.0640 \\ 0.0640 \\ 0.0757 \\ 0.0886 \\ 0.0959 \\ 0.1041 \\ 0.1041 \\ 0.1543 \\ 0.1814 \\ 0.1864 \end{bmatrix})$$

Conducting exponential regression analysis, the coefficients for the line 8-5 outage case are $a_7 = 353.749$, $b_7 = -22.494$. The estimated exponential relationship between $[|\mathrm{LODF}|]_7$ and $[\mathrm{x}]_7$ is presented as:

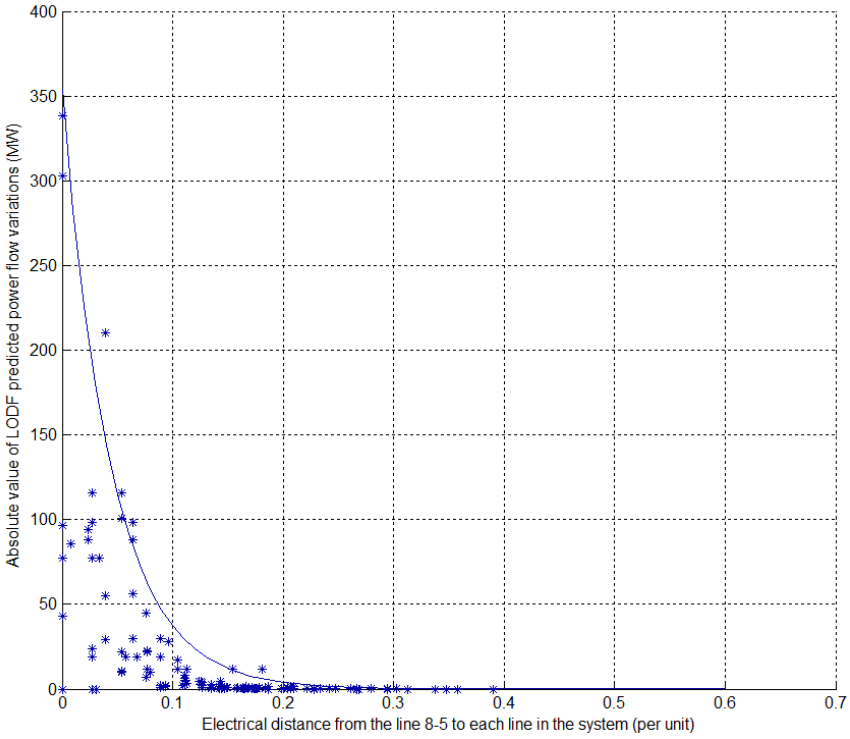

Figure 3. 18: Exponential regression result of line 8-5 outage case

As can be seen in the figure, the fitted exponential curve estimates the convergence of maximum possible LODF predicted power variations against electrical distances very well.

The same analysis is conducted to line 38-37 outage case in the IEEE 118 bus system. The index of line 38-37 outage is *i*=49. The relationship between the absolute value of LODF predicted power flow variations of each line and electrical distances from line 38-37 to each line in the system is shown in Figure 3.14. For this line outage case, 13 boundary points are selected from the data, and the exponential regression model becomes:

$$[|\mathrm{LODF}|]_{49} = a_{49} * \exp(\mathrm{b}_{49} * [\mathrm{x}]_{49}) \qquad (3.5.3)$$

Conducting exponential regression analysis, the coefficients $a_{49} = 241.983$, $b_{49} = -26.336$ are for line 38-37 outage case. The estimated exponential relation between $[|\mathrm{LODF}|]_{49}$ and $[\mathrm{x}]_{49}$ is presented as:

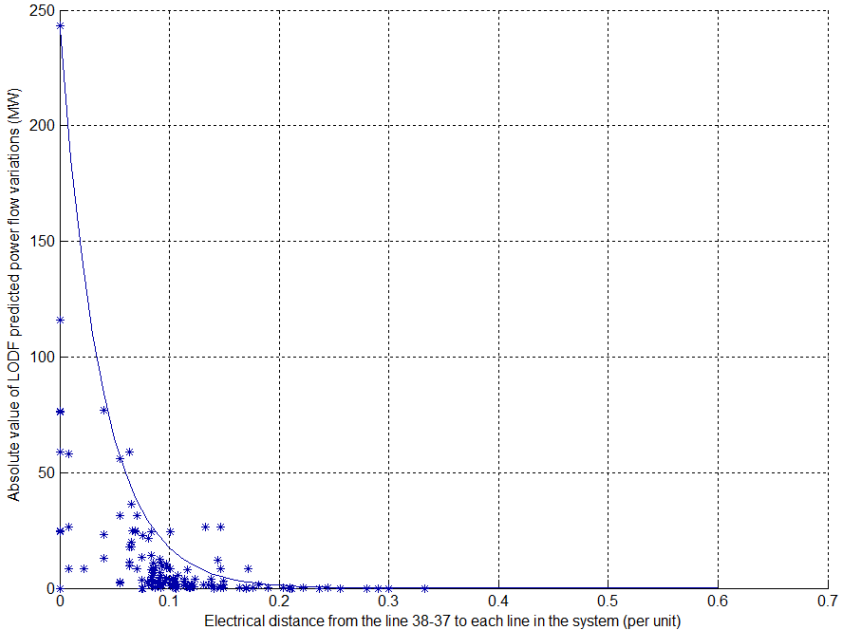

Figure 3. 19: Exponential regression result of line 38-37 outage case

As previous, the convergence of maximum possible LODF predicted power variations against electrical distances is well estimated by the exponential fitting curve.

The same exponential regression process was applied to all 176 possible contingency cases. The result can be seen below in Figure 3.20. :

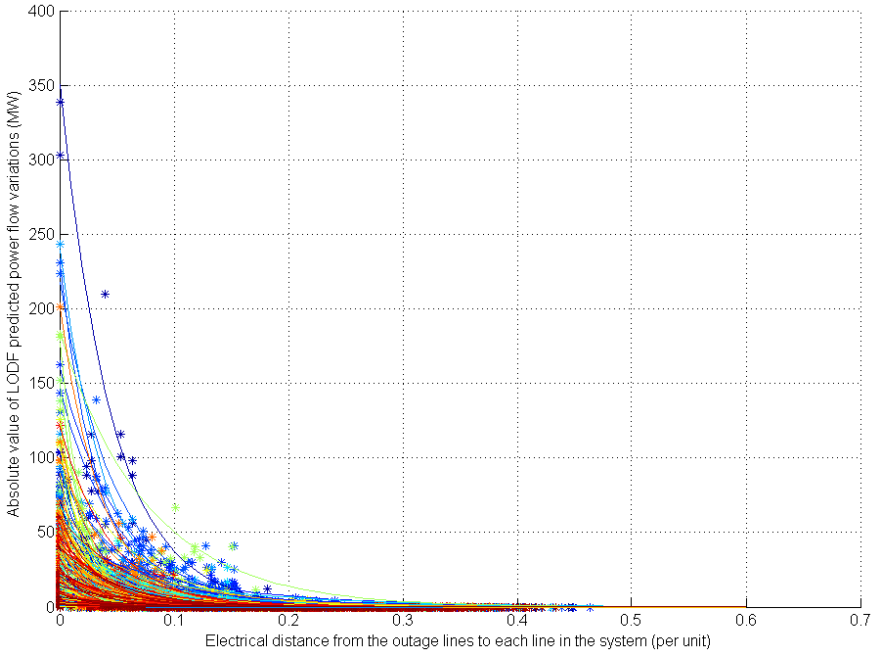

Figure 3. 20: Exponential regression estimation results of all 176 line outage cases

Each color corresponds to a line outage case in Figure 3.20. As can be seen in the figure, each one from all the 176 curves of power flow variations starts differently between 0.79 MW and 353.75 MW due the different capacities on different outage lines, gradually dropping to less than 50 MW when electrical distance increases to 0.1 per unit and eventually to a negligible value when electrical distance increases to over 0.2 per unit.

The statistic information of aggression analysis result are shown below:

Power Flow Variations	Number of Outage Cases	Percentage
0 to 10 MW	156	88.6%
10 to 20 MW	15	8.5%
20 to 30 MW	3	1.7%
30 to 40 MW	1	0.6%
40 to 50 MW	0	0.0%
50 to 60 MW	1	0.6%

Table 3. 1: The impact of line outage on active power flow variations when electrical distance increases to 0.1 per unit

Furthest Electrical Distance	Number of Outage Cases	Percentage
0 to 0.05 p.u	106	60.2%
0.05 to 0.1 p.u	50	28.4%
0.1 to 0.15 p.u	17	9.7%
0.15 to 0.2 p.u	2	1.1%
0.2 to 0.25 p.u	1	0.6%

Table 3. 2: The furthest electrical distance the impact of line outage can reach in IEEE 118 bus system

As can be seen in Table 3.1, the impacts of 88.6% of line contingencies decay to under 10 MW at 0.1 p.u. Only one line outage case has an impact between 50-60 MW at 0.1 p.u. In Table 3.2, the impacts of 60.2% of line outage cases die off before 0.05 p.u. Another 28.4% cases reach 0.05-0.1 p.u. There is only one line outage case whose impact can reach over 0.2 p.u, with the furthest affected distance is predicted as 0.21 p.u.

Therefore, the furthest electrical distance a single line outage can reach is predicted as 0.21 per unit, which means any line beyond this distance does not need to be monitored when a line outage happens in IEEE 118 bus system.

The exponential regression coefficients a_i and b_i for the 176 line outage cases are shown as follows:

Outage Line Index	a_i	b_i
1	12.82	-25.30
2	38.88	-28.15
3	103.78	-43.16
4	71.66	-33.84
5	93.14	-33.17
6	37.05	-30.08
8	353.75	-22.49
10	62.28	-61.94
11	74.80	-58.95
12	34.63	-32.47
13	32.87	-44.44
14	9.91	-39.93
15	16.04	-50.80

Outage Line Index	a_i	b_i
62	36.91	-11.62
63	31.60	-17.96
64	14.86	-21.64
65	9.50	-24.05
66	62.64	-18.60
67	62.64	-18.60
68	49.82	-20.03
69	36.39	-16.89
70	54.53	-21.61
71	68.95	-23.93
72	29.72	-16.23
73	11.07	-11.87
74	12.82	-23.81

Outage Line Index	a_i	b_i
123	91.79	-65.76
124	43.60	-103.68
125	64.61	-60.46
126	44.33	-32.71
127	45.32	-43.35
128	3.01	-26.37
129	50.54	-12.03
130	23.83	-27.60
131	41.74	-27.33
132	36.84	-20.94
135	51.36	-20.41
136	72.55	-22.00
137	99.77	-22.25

16	36.11	-20.41
17	18.84	-20.74
18	0.79	-20.77
19	4.39	-20.83
20	7.90	-20.45
21	104.04	-29.53
22	18.01	-20.42
23	83.19	-30.12
24	19.65	-28.63
25	10.79	-14.73
26	11.80	-20.37
27	30.04	-8.99
28	44.49	-8.93
29	54.96	-13.18
30	8.68	-8.81
31	160.92	-18.92
32	90.39	-17.55
33	146.48	-19.94
34	34.44	-16.72
35	16.04	-15.34
36	231.19	-29.81
37	74.74	-29.56
38	219.77	-20.77
39	14.15	-21.31
40	8.63	-17.21
41	92.13	-19.09
42	29.86	-21.05
43	12.90	-26.52
44	7.72	-17.02
45	3.67	-24.44
46	0.88	-41.43
47	33.84	-449.65
48	16.11	-17.97
49	30.25	-467.97
50	97.02	-36.99
51	241.98	-26.34
52	54.30	-46.01
53	43.41	-45.15
54	61.84	-20.38
55	26.91	-18.22
75	37.66	-31.01
76	37.63	-31.03
77	7.07	-59.49
78	18.53	-31.84
79	21.42	-53.54
80	23.05	-25.51
81	36.75	-14.49
82	6.94	-16.16
83	19.54	-15.30
84	30.31	-44.33
85	27.90	-46.15
86	29.25	-45.87
87	34.40	-44.72
88	42.45	-38.09
89	53.10	-45.55
90	111.56	-75.49
91	9.84	-61.85
92	25.22	-61.41
93	150.93	-45.57
94	151.45	-49.70
95	31.05	-47.78
96	184.24	-12.95
97	180.14	-50.83
98	131.40	-60.03
99	131.40	-60.03
100	37.42	-55.48
101	25.14	-30.25
102	8.46	-40.13
103	55.31	-31.39
104	13.79	-32.56
105	58.54	-28.16
106	48.52	-31.43
107	125.35	-43.52
108	106.18	-16.52
109	5.87	-13.00
110	17.25	-9.92
112	11.00	-9.06
114	16.09	-45.37
115	0.13	-29.73
116	108.18	-42.72
138	58.30	-41.49
139	112.46	-32.42
140	1.46	-19.21
141	202.93	-27.86
142	63.59	-37.33
143	9.11	-28.48
144	58.28	-29.10
145	52.36	-31.10
146	44.74	-25.07
147	40.49	-37.82
148	18.72	-41.98
149	9.86	-24.19
150	19.71	-47.70
151	25.09	-28.25
152	29.75	-19.14
153	20.08	-19.40
154	31.48	-30.07
155	4.29	-27.17
156	1.36	-43.42
157	11.22	-33.88
158	5.30	-22.36
159	22.86	-22.37
160	16.56	-25.48
161	46.38	-22.41
162	40.17	-17.23
163	121.43	-22.88
164	56.17	-48.43
165	32.40	-54.42
166	43.45	-21.15
167	60.98	-16.68
168	48.21	-24.99
169	8.90	-28.25
170	26.77	-47.93
171	24.05	-22.58
172	24.00	-30.74
173	22.06	-17.28
174	60.76	-30.92
175	13.94	-14.77
178	2.07	-17.82
179	3.88	-18.76

56	15.46	-17.77	117	52.07	-26.45	180	9.31	-37.87
57	11.84	-17.67	118	61.34	-29.51	181	20.77	-29.61
58	21.60	-14.92	119	65.20	-30.79	182	1.39	-22.21
59	17.98	-7.88	120	34.60	-33.61	185	40.08	-20.00
60	1.48	-11.74	121	45.40	-49.77	186	6.65	-16.49
61	34.62	-8.31	122	25.15	-81.84			

Table 3. 3: Exponential regression coefficients for all 176 line outage cases

With the knowledge of these 176 sets of regression coefficients and the information Z bus matrix of the system which is used to calculate electrical distances of transmission lines, the maximum possible active power variation on each line due to the outage of any line in the system can be predicted directly when a line outage happens in the system.

Also, the furthest electrical distance of impact of a certain line outage can be obtained. Any line beyond this distance is not required to be considered to be monitored when the line outage happens.

3.6 Accuracy of Exponential Regression Method

To determine how the exponential regression curves fit the maximum possible power flow variations against electrical distance, the parameter coefficient of determination, R^2, is introduced in this section. R^2 is a statistics parameter which is used to measure how well the data are fitted with the regression model. It is indicative of the variance between the dependent variables predicted by model and actual values. The value of R^2 varies from 0 to 1. R^2 =1 shows that the regression model can predict the dependent variables with very high accuracy while R^2 =0 indicates that the model should not be used to predict the dependent variables at all. R^2 between 0 and 1 gives the percentage of how well the model can be used to predict the dependent variables. The larger the value of R^2 is, the better the model is able to predict the dependent variables.

The equation of the coefficient of determination for outage of line *i* is:

Outage Line Index	MW Loss from Lines	R_i^2
1	12.35	0.97
2	38.65	0.98
3	103.23	0.99
4	68.11	0.95
5	88.47	0.95
6	35.54	0.96
8	338.47	0.94
10	64.23	0.95
11	77.22	0.95
12	34.29	1.00
13	32.45	0.92
14	9.79	0.96
15	16.48	0.97
16	35.09	0.95
17	18.31	0.94
18	0.77	0.83
19	4.24	0.93
20	7.51	0.92
21	103.86	1.00
22	17.51	0.90
23	80.27	0.88
24	19.39	0.93
25	10.62	0.94
26	11.53	0.99
27	28.67	0.92
28	42.84	0.93
29	53.26	0.93
30	8.28	0.68
31	162.56	0.98
32	90.29	0.97
33	143.52	0.98
34	32.88	0.98
35	15.66	0.97
36	231.19	0.99
37	74.16	0.97
62	36.33	0.99
63	31.11	0.98
64	14.76	0.97
65	9.54	0.98
66	64.87	0.95
67	64.87	0.95
68	49.70	0.98
69	34.90	0.96
70	53.66	0.96
71	66.63	0.84
72	28.56	0.88
73	10.37	0.87
74	12.68	0.85
75	37.77	0.99
76	37.74	0.99
77	7.07	1.00
78	18.53	1.00
79	21.42	1.00
80	22.99	1.00
81	35.88	0.97
82	6.67	0.93
83	18.79	0.94
84	30.38	1.00
85	27.96	1.00
86	29.31	1.00
87	34.52	0.99
88	43.32	0.96
89	51.72	0.97
90	112.07	0.99
91	9.87	0.99
92	25.49	0.98
93	151.77	0.95
94	151.77	0.98
95	30.54	0.99
96	181.28	0.97
123	96.57	0.95
124	44.37	0.95
125	64.74	1.00
126	44.15	0.91
127	44.20	0.94
128	3.03	1.00
129	47.22	0.89
130	24.79	0.94
131	42.77	0.97
132	36.35	0.98
135	50.39	0.97
136	71.24	0.95
137	98.93	0.92
138	58.22	1.00
139	110.83	0.99
140	1.41	0.89
141	201.54	0.97
142	63.59	0.99
143	8.60	0.94
144	57.62	0.96
145	52.17	0.99
146	44.72	0.99
147	40.86	0.99
148	18.97	0.99
149	9.94	0.99
150	19.79	0.99
151	26.42	0.95
152	28.95	0.94
153	19.56	0.94
154	31.50	0.99
155	4.28	0.96
156	1.38	0.98
157	11.10	0.98
158	5.26	0.97
159	22.65	0.96

38	223.71	0.94	97	182.79	0.95	160	16.74	0.98
39	14.77	0.96	98	132.22	0.98	161	44.65	0.94
40	8.42	0.96	99	132.22	0.98	162	38.98	0.87
41	92.98	0.98	100	37.16	0.89	163	121.75	0.96
42	29.86	0.99	101	24.30	0.89	164	56.18	0.99
43	12.53	0.95	102	8.54	0.99	165	32.45	0.97
44	7.31	0.93	103	53.16	0.87	166	43.35	1.00
45	3.59	0.94	104	14.18	0.90	167	60.36	1.00
46	0.84	0.75	105	55.94	0.95	168	48.58	0.99
47	33.84	1.00	106	46.54	0.93	169	8.86	0.96
48	15.72	0.96	107	125.80	0.99	170	26.75	1.00
49	30.25	1.00	108	108.38	0.98	171	23.97	1.00
50	94.31	0.89	109	6.22	0.92	172	23.98	1.00
51	243.37	0.98	110	16.65	0.91	173	21.77	0.96
52	54.91	0.96	112	10.60	0.90	174	60.60	0.91
53	44.02	0.96	114	16.21	0.95	175	13.71	0.95
54	62.35	0.98	115	0.13	0.98	178	2.06	0.97
55	26.92	1.00	116	110.01	0.97	179	4.12	0.96
56	15.45	1.00	117	51.99	0.97	180	9.37	0.98
57	11.84	1.00	118	61.15	0.98	181	20.72	0.99
58	21.59	0.99	119	62.21	0.96	182	1.36	0.89
59	16.59	0.75	120	34.61	0.96	185	40.21	0.99
60	1.41	0.85	121	45.39	1.00	186	6.85	0.98
61	32.77	0.76	122	25.68	0.92			

Table 3. 4: Calculated results of coefficient of determination for all 176 line outage cases

$$\mathrm{R}_i{}^2 = 1 - \frac{SS_{res}}{SS_{tot}} \tag{3.6.1}$$

SS_{tol} is the sum of the squares of the difference between actual dependent variables and their mean values. Its equation is:

$$SS_{tot} = \sum_{m=1}^{186}(|\mathrm{LODF}_m|_i - \overline{|\mathrm{LODF}|}_i)^2 \tag{3.6.2}$$

SS_{res} is the sum of squares of residuals of the difference between the data and the model predicted values. The equation to calculate SS_{res} is:

$$SS_{tot} = \sum_{m=1}^{186}(|\mathrm{LODF}_m|_i - |\widehat{\mathrm{LODF}}_m|_i)^2 \tag{3.6.3}$$

Where 186 is both the total number of branches in the system and the total number of data points for one line outage case. $|\widehat{\mathrm{LODF}_m}|_\iota$ is the model predicted value of power flow variation of the m^{th} branch when the i^{th} branch is tripped.

Since the value of R^2 corresponds with a single line outage case and there are 176 possible outage cases in the IEEE 118 bus system, the 176 R_i^2 values are calculated as follows:

The statistics information of the distribution of coefficient of determination is shown in Table 3.5:

Interval of R_i^2	Count	Percentage
(0.9-1.0)	156	88.64%
(0.8-0.9)	16	9.10%
(0.7-0.8)	3	1.70%
(0.6-0.7)	1	0.57%

Table 3. 5: Statistics information of coefficient of determination

As can be seen in Table 3.5, for all of the 176 possible line outage cases, 88.64% of cases have R^2 values larger than 0.9. This indicates that their maximum boundaries of the absolute value of LODF predicted power flow variations against electrical distances could be well predicted by the exponential regression model. Additionally, 9.1% cases have R^2 values larger than 0.8, which is still a good accuracy for the prediction model. Only 3 cases have R^2 values range between 0.7 and 0.8 with one case lower than 0.7.

For the heavy-loaded line outage cases, neighboring transmission lines have higher chances to be overloaded. Thus, the accuracy of exponential regression model to predict maximum possible LODF predicted power flow variations caused by outage of heavy-loaded line is more important. The data of R_i^2 for line outage cases with a loss more than 100 MW are shown in Table 3.6:

Outage Line Index	MW Loss from Lines	R_i^2
3	103.23	0.99
8	338.47	0.94
21	103.86	1.00
31	162.56	0.98
33	143.52	0.98
36	231.19	0.99
38	223.71	0.94
51	243.37	0.98
90	112.07	0.99
93	151.77	0.95
94	151.77	0.98
96	181.28	0.97
97	182.79	0.95
98	132.22	0.98
99	132.22	0.98
107	125.8	0.99
108	108.38	0.98
116	110.01	0.97
139	110.83	0.99
141	201.54	0.97
163	121.75	0.96

Table 3. 6: Coefficients of determination of heavy-loaded line outage cases

As can been seen in Table 3.6, all of R_i^2 values for heavy loaded lines are greater than 0.94. Therefore, the exponential regression prediction model performs well in predicting the convergence tendency of the maximum possible power flow variations against electrical distances for the significant lines in the IEEE 118 bus system.

3.7 Summary

In this chapter, the Line Outage Distribution Factor (LODF) algorithm and Thevenin electrical distance algorithm has been introduced and implemented in the IEEE 118 bus system. Then, following the analysis of the impact of the line outage contingency with a DC load flow algorithm in the IEEE 118 bus system, a convergence tendency has been found between the maximum possible absolute value of LODF of each line and the electrical distances between the outage lines and each line in the system. After that, exponential regression was done to estimate the convergence tendency of the maximum possible LODF predicted power flow variations against electrical distances. Also, the accuracy of the model has been analyzed. The result shows that the fitted curves created by the regression model perform well in estimating the relationship between the maximum possible LODF predicted power flow variations and the electrical distances. With the parameters of these fitted curves, the maximum possible power variation on each line and the furthest electrical distance the impact of single line outage can reach in the system can be quickly predicted when a single line outage happens.

Chapter 4: Conclusion and Future Scope of Work

4.1 Conclusion

Several examples of large-scale blackouts in Chapter 1 illustrate that the loss of significant elements in the power system, such as transmission lines, will bring about serious negative impacts and damage to the system. Without timely corrective response, a single line outage contingency can cause one or several other transmission lines to overload and can lead to a cascading failure.

This work performs a line outage contingency analysis using LODF method as well as a detailed analysis of post-contingency bus voltage angle variations and line power flow variations in the IEEE 118 bus system. After that, an approximation of electrical distance between two transmission lines is derived from the Thevenin electrical distance between two nodes. Combining the information of the LODF and the electrical distances, a convergence relationship has been found between the maximum possible LODF predicted power flow variation and electrical distance from the outage line to each line in the system, which satisfies all possible line outage cases in the system. Then, an exponential regression analysis was done to estimate this convergence relationship.

The major contribution of this thesis is an exponential convergence relationship is found between the maximum possible power flow variations and electrical distances from the outage line to each line in the system. With only the result of regression coefficients and the information of the system impedance matrix, which is used to estimate the LODF values and the electrical distances between lines, both the maximum possible power flow variation on each line in the system and the furthest electrical distance that each line outage impact can reach can be estimated quickly.

If this analysis method can be applied in a practical system, it will help the system operator find out quickly and accurately which line will be a potential risk to be overloaded and which line will not be affected when a line outage happens.

4.2 Future Scope of Work

In this thesis, only the single line outage case has been analyzed. However, the conclusion should be expanded to analyzing the impact of two or several lines outage cases. In addition, the analysis is only conducted in the IEEE 118 bus system positive sequence network whereas the practical power system is not only operated in the positive sequence. For the three-phase unbalanced system, the accuracy and correctness of the conclusion still needs to be studied. Also, more practical system should be tested in the future.

Appendix

Bus Data

Bus No.	Bus Type	Pd (MW)	Qd (MVAR)	Vm (p.u)	Va (p.u)	BaseKV	Vmax (p.u)	Vmin (p.u)
1	2	51	27	0.955	10.67	138	1.06	0.94
2	1	20	9	0.971	11.22	138	1.06	0.94
3	1	39	10	0.968	11.56	138	1.06	0.94
4	2	39	12	0.998	15.28	138	1.06	0.94
5	1	0	0	1.002	15.73	138	1.06	0.94
6	2	52	22	0.99	13	138	1.06	0.94
7	1	19	2	0.989	12.56	138	1.06	0.94
8	2	28	0	1.015	20.77	345	1.06	0.94
9	1	0	0	1.043	28.02	345	1.06	0.94
10	2	0	0	1.05	35.61	345	1.06	0.94
11	1	70	23	0.985	12.72	138	1.06	0.94
12	2	47	10	0.99	12.2	138	1.06	0.94
13	1	34	16	0.968	11.35	138	1.06	0.94
14	1	14	1	0.984	11.5	138	1.06	0.94
15	2	90	30	0.97	11.23	138	1.06	0.94
16	1	25	10	0.984	11.91	138	1.06	0.94
17	1	11	3	0.995	13.74	138	1.06	0.94
18	2	60	34	0.973	11.53	138	1.06	0.94
19	2	45	25	0.963	11.05	138	1.06	0.94
20	1	18	3	0.958	11.93	138	1.06	0.94
21	1	14	8	0.959	13.52	138	1.06	0.94
22	1	10	5	0.97	16.08	138	1.06	0.94
23	1	7	3	1	21	138	1.06	0.94
24	2	13	0	0.992	20.89	138	1.06	0.94

25	2	0	0	1.05	27.93	138	1.06	0.94
26	2	0	0	1.015	29.71	345	1.06	0.94
27	2	71	13	0.968	15.35	138	1.06	0.94
28	1	17	7	0.962	13.62	138	1.06	0.94
29	1	24	4	0.963	12.63	138	1.06	0.94
30	1	0	0	0.968	18.79	345	1.06	0.94
31	2	43	27	0.967	12.75	138	1.06	0.94
32	2	59	23	0.964	14.8	138	1.06	0.94
33	1	23	9	0.972	10.63	138	1.06	0.94
34	2	59	26	0.986	11.3	138	1.06	0.94
35	1	33	9	0.981	10.87	138	1.06	0.94
36	2	31	17	0.98	10.87	138	1.06	0.94
37	1	0	0	0.992	11.77	138	1.06	0.94
38	1	0	0	0.962	16.91	345	1.06	0.94
39	1	27	11	0.97	8.41	138	1.06	0.94
40	2	66	23	0.97	7.35	138	1.06	0.94
41	1	37	10	0.967	6.92	138	1.06	0.94
42	2	96	23	0.985	8.53	138	1.06	0.94
43	1	18	7	0.978	11.28	138	1.06	0.94
44	1	16	8	0.985	13.82	138	1.06	0.94
45	1	53	22	0.987	15.67	138	1.06	0.94
46	2	28	10	1.005	18.49	138	1.06	0.94
47	1	34	0	1.017	20.73	138	1.06	0.94
48	1	20	11	1.021	19.93	138	1.06	0.94
49	2	87	30	1.025	20.94	138	1.06	0.94
50	1	17	4	1.001	18.9	138	1.06	0.94
51	1	17	8	0.967	16.28	138	1.06	0.94
52	1	18	5	0.957	15.32	138	1.06	0.94
53	1	23	11	0.946	14.35	138	1.06	0.94
54	2	113	32	0.955	15.26	138	1.06	0.94
55	2	63	22	0.952	14.97	138	1.06	0.94
56	2	84	18	0.954	15.16	138	1.06	0.94

57	1	12	3	0.971	16.36	138	1.06	0.94
58	1	12	3	0.959	15.51	138	1.06	0.94
59	2	277	113	0.985	19.37	138	1.06	0.94
60	1	78	3	0.993	23.15	138	1.06	0.94
61	2	0	0	0.995	24.04	138	1.06	0.94
62	2	77	14	0.998	23.43	138	1.06	0.94
63	1	0	0	0.969	22.75	345	1.06	0.94
64	1	0	0	0.984	24.52	345	1.06	0.94
65	2	0	0	1.005	27.65	345	1.06	0.94
66	2	39	18	1.05	27.48	138	1.06	0.94
67	1	28	7	1.02	24.84	138	1.06	0.94
68	1	0	0	1.003	27.55	345	1.06	0.94
69	3	0	0	1.035	30	138	1.06	0.94
70	2	66	20	0.984	22.58	138	1.06	0.94
71	1	0	0	0.987	22.15	138	1.06	0.94
72	2	12	0	0.98	20.98	138	1.06	0.94
73	2	6	0	0.991	21.94	138	1.06	0.94
74	2	68	27	0.958	21.64	138	1.06	0.94
75	1	47	11	0.967	22.91	138	1.06	0.94
76	2	68	36	0.943	21.77	138	1.06	0.94
77	2	61	28	1.006	26.72	138	1.06	0.94
78	1	71	26	1.003	26.42	138	1.06	0.94
79	1	39	32	1.009	26.72	138	1.06	0.94
80	2	130	26	1.04	28.96	138	1.06	0.94
81	1	0	0	0.997	28.1	345	1.06	0.94
82	1	54	27	0.989	27.24	138	1.06	0.94
83	1	20	10	0.985	28.42	138	1.06	0.94
84	1	11	7	0.98	30.95	138	1.06	0.94
85	2	24	15	0.985	32.51	138	1.06	0.94
86	1	21	10	0.987	31.14	138	1.06	0.94
87	2	0	0	1.015	31.4	161	1.06	0.94
88	1	48	10	0.987	35.64	138	1.06	0.94

89	2	0	0	1.005	39.69	138	1.06	0.94
90	2	163	42	0.985	33.29	138	1.06	0.94
91	2	10	0	0.98	33.31	138	1.06	0.94
92	2	65	10	0.993	33.8	138	1.06	0.94
93	1	12	7	0.987	30.79	138	1.06	0.94
94	1	30	16	0.991	28.64	138	1.06	0.94
95	1	42	31	0.981	27.67	138	1.06	0.94
96	1	38	15	0.993	27.51	138	1.06	0.94
97	1	15	9	1.011	27.88	138	1.06	0.94
98	1	34	8	1.024	27.4	138	1.06	0.94
99	2	42	0	1.01	27.04	138	1.06	0.94
100	2	37	18	1.017	28.03	138	1.06	0.94
101	1	22	15	0.993	29.61	138	1.06	0.94
102	1	5	3	0.991	32.3	138	1.06	0.94
103	2	23	16	1.001	24.44	138	1.06	0.94
104	2	38	25	0.971	21.69	138	1.06	0.94
105	2	31	26	0.965	20.57	138	1.06	0.94
106	1	43	16	0.962	20.32	138	1.06	0.94
107	2	50	12	0.952	17.53	138	1.06	0.94
108	1	2	1	0.967	19.38	138	1.06	0.94
109	1	8	3	0.967	18.93	138	1.06	0.94
110	2	39	30	0.973	18.09	138	1.06	0.94
111	2	0	0	0.98	19.74	138	1.06	0.94
112	2	68	13	0.975	14.99	138	1.06	0.94
113	2	6	0	0.993	13.74	138	1.06	0.94
114	1	8	3	0.96	14.46	138	1.06	0.94
115	1	22	7	0.96	14.46	138	1.06	0.94
116	2	184	0	1.005	27.12	138	1.06	0.94
117	1	20	8	0.974	10.67	138	1.06	0.94
118	1	33	15	0.949	21.92	138	1.06	0.94

Generator Data

Bus No.	Pg (MW)	Qg (MVAR)	Qmax (MVAR)	Qmin (MVAR)	Vg (p.u)	mBase (MVA)	Pmax (MW)	Pmin (MW)
1	0	0	15	-5	0.955	100	100	0
4	0	0	300	-300	0.998	100	100	0
6	0	0	50	-13	0.99	100	100	0
8	0	0	300	-300	1.015	100	100	0
10	450	0	200	-147	1.05	100	550	0
12	85	0	120	-35	0.99	100	185	0
15	0	0	30	-10	0.97	100	100	0
18	0	0	50	-16	0.973	100	100	0
19	0	0	24	-8	0.962	100	100	0
24	0	0	300	-300	0.992	100	100	0
25	220	0	140	-47	1.05	100	320	0
26	314	0	1000	-1000	1.015	100	414	0
27	0	0	300	-300	0.968	100	100	0
31	7	0	300	-300	0.967	100	107	0
32	0	0	42	-14	0.963	100	100	0
34	0	0	24	-8	0.984	100	100	0
36	0	0	24	-8	0.98	100	100	0
40	0	0	300	-300	0.97	100	100	0
42	0	0	300	-300	0.985	100	100	0
46	19	0	100	-100	1.005	100	119	0
49	204	0	210	-85	1.025	100	304	0
54	48	0	300	-300	0.955	100	148	0
55	0	0	23	-8	0.952	100	100	0
56	0	0	15	-8	0.954	100	100	0
59	155	0	180	-60	0.985	100	255	0
61	160	0	300	-100	0.995	100	260	0
62	0	0	20	-20	0.998	100	100	0
65	391	0	200	-67	1.005	100	491	0
66	392	0	200	-67	1.05	100	492	0

69	516.4	0	300	-300	1.035	100	805.2	0
70	0	0	32	-10	0.984	100	100	0
72	0	0	100	-100	0.98	100	100	0
73	0	0	100	-100	0.991	100	100	0
74	0	0	9	-6	0.958	100	100	0
76	0	0	23	-8	0.943	100	100	0
77	0	0	70	-20	1.006	100	100	0
80	477	0	280	-165	1.04	100	577	0
85	0	0	23	-8	0.985	100	100	0
87	4	0	1000	-100	1.015	100	104	0
89	607	0	300	-210	1.005	100	707	0
90	0	0	300	-300	0.985	100	100	0
91	0	0	100	-100	0.98	100	100	0
92	0	0	9	-3	0.99	100	100	0
99	0	0	100	-100	1.01	100	100	0
100	252	0	155	-50	1.017	100	352	0
103	40	0	40	-15	1.01	100	140	0
104	0	0	23	-8	0.971	100	100	0
105	0	0	23	-8	0.965	100	100	0
107	0	0	200	-200	0.952	100	100	0
110	0	0	23	-8	0.973	100	100	0
111	36	0	1000	-100	0.98	100	136	0
112	0	0	1000	-100	0.975	100	100	0
113	0	0	200	-100	0.993	100	100	0
116	0	0	1000	-1000	1.005	100	100	0

Branch Data

Branch No.	From bus	To bus	R (p.u)	X (p.u)	B (p.u)
1	1	2	0.0303	0.0999	0.0254
2	1	3	0.0129	0.0424	0.01082
3	4	5	0.00176	0.00798	0.0021
4	3	5	0.0241	0.108	0.0284
5	5	6	0.0119	0.054	0.01426
6	6	7	0.00459	0.0208	0.0055
7	8	9	0.00244	0.0305	1.162
8	8	5	0	0.0267	0
9	9	10	0.00258	0.0322	1.23
10	4	11	0.0209	0.0688	0.01748
11	5	11	0.0203	0.0682	0.01738
12	11	12	0.00595	0.0196	0.00502
13	2	12	0.0187	0.0616	0.01572
14	3	12	0.0484	0.16	0.0406
15	7	12	0.00862	0.034	0.00874
16	11	13	0.02225	0.0731	0.01876
17	12	14	0.0215	0.0707	0.01816
18	13	15	0.0744	0.2444	0.06268
19	14	15	0.0595	0.195	0.0502
20	12	16	0.0212	0.0834	0.0214
21	15	17	0.0132	0.0437	0.0444
22	16	17	0.0454	0.1801	0.0466
23	17	18	0.0123	0.0505	0.01298
24	18	19	0.01119	0.0493	0.01142
25	19	20	0.0252	0.117	0.0298
26	15	19	0.012	0.0394	0.0101
27	20	21	0.0183	0.0849	0.0216
28	21	22	0.0209	0.097	0.0246
29	22	23	0.0342	0.159	0.0404

30	23	24	0.0135	0.0492	0.0498
31	23	25	0.0156	0.08	0.0864
32	26	25	0	0.0382	0
33	25	27	0.0318	0.163	0.1764
34	27	28	0.01913	0.0855	0.0216
35	28	29	0.0237	0.0943	0.0238
36	30	17	0	0.0388	0
37	8	30	0.00431	0.0504	0.514
38	26	30	0.00799	0.086	0.908
39	17	31	0.0474	0.1563	0.0399
40	29	31	0.0108	0.0331	0.0083
41	23	32	0.0317	0.1153	0.1173
42	31	32	0.0298	0.0985	0.0251
43	27	32	0.0229	0.0755	0.01926
44	15	33	0.038	0.1244	0.03194
45	19	34	0.0752	0.247	0.0632
46	35	36	0.00224	0.0102	0.00268
47	35	37	0.011	0.0497	0.01318
48	33	37	0.0415	0.142	0.0366
49	34	36	0.00871	0.0268	0.00568
50	34	37	0.00256	0.0094	0.00984
51	38	37	0	0.0375	0
52	37	39	0.0321	0.106	0.027
53	37	40	0.0593	0.168	0.042
54	30	38	0.00464	0.054	0.422
55	39	40	0.0184	0.0605	0.01552
56	40	41	0.0145	0.0487	0.01222
57	40	42	0.0555	0.183	0.0466
58	41	42	0.041	0.135	0.0344
59	43	44	0.0608	0.2454	0.06068
60	34	43	0.0413	0.1681	0.04226
61	44	45	0.0224	0.0901	0.0224

62	45	46	0.04	0.1356	0.0332
63	46	47	0.038	0.127	0.0316
64	46	48	0.0601	0.189	0.0472
65	47	49	0.0191	0.0625	0.01604
66	42	49	0.0715	0.323	0.086
67	42	49	0.0715	0.323	0.086
68	45	49	0.0684	0.186	0.0444
69	48	49	0.0179	0.0505	0.01258
70	49	50	0.0267	0.0752	0.01874
71	49	51	0.0486	0.137	0.0342
72	51	52	0.0203	0.0588	0.01396
73	52	53	0.0405	0.1635	0.04058
74	53	54	0.0263	0.122	0.031
75	49	54	0.073	0.289	0.0738
76	49	54	0.0869	0.291	0.073
77	54	55	0.0169	0.0707	0.0202
78	54	56	0.00275	0.00955	0.00732
79	55	56	0.00488	0.0151	0.00374
80	56	57	0.0343	0.0966	0.0242
81	50	57	0.0474	0.134	0.0332
82	56	58	0.0343	0.0966	0.0242
83	51	58	0.0255	0.0719	0.01788
84	54	59	0.0503	0.2293	0.0598
85	56	59	0.0825	0.251	0.0569
86	56	59	0.0803	0.239	0.0536
87	55	59	0.04739	0.2158	0.05646
88	59	60	0.0317	0.145	0.0376
89	59	61	0.0328	0.15	0.0388
90	60	61	0.00264	0.0135	0.01456
91	60	62	0.0123	0.0561	0.01468
92	61	62	0.00824	0.0376	0.0098
93	63	59	0	0.0386	0

94	63	64	0.00172	0.02	0.216
95	64	61	0	0.0268	0
96	38	65	0.00901	0.0986	1.046
97	64	65	0.00269	0.0302	0.38
98	49	66	0.018	0.0919	0.0248
99	49	66	0.018	0.0919	0.0248
100	62	66	0.0482	0.218	0.0578
101	62	67	0.0258	0.117	0.031
102	65	66	0	0.037	0
103	66	67	0.0224	0.1015	0.02682
104	65	68	0.00138	0.016	0.638
105	47	69	0.0844	0.2778	0.07092
106	49	69	0.0985	0.324	0.0828
107	68	69	0	0.037	0
108	69	70	0.03	0.127	0.122
109	24	70	0.00221	0.4115	0.10198
110	70	71	0.00882	0.0355	0.00878
111	24	72	0.0488	0.196	0.0488
112	71	72	0.0446	0.18	0.04444
113	71	73	0.00866	0.0454	0.01178
114	70	74	0.0401	0.1323	0.03368
115	70	75	0.0428	0.141	0.036
116	69	75	0.0405	0.122	0.124
117	74	75	0.0123	0.0406	0.01034
118	76	77	0.0444	0.148	0.0368
119	69	77	0.0309	0.101	0.1038
120	75	77	0.0601	0.1999	0.04978
121	77	78	0.00376	0.0124	0.01264
122	78	79	0.00546	0.0244	0.00648
123	77	80	0.017	0.0485	0.0472
124	77	80	0.0294	0.105	0.0228
125	79	80	0.0156	0.0704	0.0187

126	68	81	0.00175	0.0202	0.808
127	81	80	0	0.037	0
128	77	82	0.0298	0.0853	0.08174
129	82	83	0.0112	0.03665	0.03796
130	83	84	0.0625	0.132	0.0258
131	83	85	0.043	0.148	0.0348
132	84	85	0.0302	0.0641	0.01234
133	85	86	0.035	0.123	0.0276
134	86	87	0.02828	0.2074	0.0445
135	85	88	0.02	0.102	0.0276
136	85	89	0.0239	0.173	0.047
137	88	89	0.0139	0.0712	0.01934
138	89	90	0.0518	0.188	0.0528
139	89	90	0.0238	0.0997	0.106
140	90	91	0.0254	0.0836	0.0214
141	89	92	0.0099	0.0505	0.0548
142	89	92	0.0393	0.1581	0.0414
143	91	92	0.0387	0.1272	0.03268
144	92	93	0.0258	0.0848	0.0218
145	92	94	0.0481	0.158	0.0406
146	93	94	0.0223	0.0732	0.01876
147	94	95	0.0132	0.0434	0.0111
148	80	96	0.0356	0.182	0.0494
149	82	96	0.0162	0.053	0.0544
150	94	96	0.0269	0.0869	0.023
151	80	97	0.0183	0.0934	0.0254
152	80	98	0.0238	0.108	0.0286
153	80	99	0.0454	0.206	0.0546
154	92	100	0.0648	0.295	0.0472
155	94	100	0.0178	0.058	0.0604
156	95	96	0.0171	0.0547	0.01474
157	96	97	0.0173	0.0885	0.024

158	98	100	0.0397	0.179	0.0476
159	99	100	0.018	0.0813	0.0216
160	100	101	0.0277	0.1262	0.0328
161	92	102	0.0123	0.0559	0.01464
162	101	102	0.0246	0.112	0.0294
163	100	103	0.016	0.0525	0.0536
164	100	104	0.0451	0.204	0.0541
165	103	104	0.0466	0.1584	0.0407
166	103	105	0.0535	0.1625	0.0408
167	100	106	0.0605	0.229	0.062
168	104	105	0.00994	0.0378	0.00986
169	105	106	0.014	0.0547	0.01434
170	105	107	0.053	0.183	0.0472
171	105	108	0.0261	0.0703	0.01844
172	106	107	0.053	0.183	0.0472
173	108	109	0.0105	0.0288	0.0076
174	103	110	0.03906	0.1813	0.0461
175	109	110	0.0278	0.0762	0.0202
176	110	111	0.022	0.0755	0.02
177	110	112	0.0247	0.064	0.062
178	17	113	0.00913	0.0301	0.00768
179	32	113	0.0615	0.203	0.0518
180	32	114	0.0135	0.0612	0.01628
181	27	115	0.0164	0.0741	0.01972
182	114	115	0.0023	0.0104	0.00276
183	68	116	0.00034	0.00405	0.164
184	12	117	0.0329	0.14	0.0358
185	75	118	0.0145	0.0481	0.01198
186	76	118	0.0164	0.0544	0.01356

Reference

[1] " Lightning knocked out Brazil power " in *BBC News*, ed, 1999-03-13. Retrieved 2009-04-07.

[2] "Final Report on the August 14, 2003 Blackout in the United States and Canada: Causes and Recommendations

" April 2014.

[3] "ERGEG Final Report The lessons to be learned from the large disturbance in the European power system on the 4th of November 2006," February 2007.

[4] W. D. S. John J. Grainger, Jr., *Power System Analysis*.

[5] Q. Huang, L. Shao, and N. Li, "Dynamic detection of transmission line outages using Hidden Markov Models," in *American Control Conference (ACC), 2015*, 2015, pp. 5050-5055.

[6] J. Chen, Y. Zhao, A. Goldsmith, and H. V. Poor, "Line outage detection in power transmission networks via message passing algorithms," in *Signals, Systems and Computers, 2014 48th Asilomar Conference on*, 2014, pp. 350-354.

[7] H. Sehwail and I. Dobson, "Locating line outages in a specific area of a power system with synchrophasors," in *North American Power Symposium (NAPS), 2012*, 2012, pp. 1-6.

[8] T. Banerjee, Y. C. Chen, A. D. Domínguez-García, and V. V. Veeravalli, "Power system line outage detection and identification-A quickest change detection approach," in *ICASSP*, 2014, pp. 3450-3454.

[9] Y. C. Chen, T. Banerjee, A. D. Domínguez-García, and V. V. Veeravalli, "Quickest line outage detection and identification," *Power Systems, IEEE Transactions on,* vol. 31, pp. 749-758, 2016.

[10] A. Abdelaziz, S. Mekhamer, M. Ezzat, and E. El-Saadany, "Line outage detection using support vector machine (SVM) based on the phasor measurement units (PMUs) technology," in *Power and Energy Society General Meeting, 2012 IEEE*, 2012, pp. 1-8.

[11] J. E. Tate and T. J. Overbye, "Double line outage detection using phasor angle measurements," in *Power & Energy Society General Meeting, 2009. PES'09. IEEE*, 2009, pp. 1-5.

[12] A. Ahmed, M. Awais, M. Naeem, M. Iqbal, and A. Alpalagan, "Efficient multiple lines outage detection in SmartGrid," in *Power Generation System and Renewable Energy Technologies (PGSRET), 2015*, 2015, pp. 1-6.

[13] J. Zare and F. Aminifar, "Synchrophasor-assisted line outage identification: A simple and iterative algorithm," in *Electrical Engineering (ICEE), 2015 23rd Iranian Conference on*, 2015, pp. 1556-1561.

[14] I. Dobson, "Estimating the propagation and extent of cascading line outages from utility data with a branching process," *Power Systems, IEEE Transactions on,* vol. 27, pp. 2146-2155, 2012.

[15] T. L. Baldwin, M. S. Tawfik, and M. McQueen, "Contingency Analysis of Cascading Line Outage Events," in *Power Systems Conference*, 2011, pp. 1-8.

[16] Y. Zhu, J. Yan, Y. Tang, Y. L. Sun, and H. He, "Diversity of cascading failure processes in electrical grids," in *Innovative Smart Grid Technologies Conference (ISGT), 2015 IEEE Power & Energy Society*, 2015, pp. 1-5.
[17] I. Dobson, "Obtaining statistics of cascading line outages spreading in an electric transmission network from standard utility data," *arXiv preprint arXiv:1507.04277,* 2015.
[18] L. N. Roman Vykuka, "Sensitivity Factors for Contingency Analysis."
[19] A. Jana, P. D. Gupta, and G. Durga Prasad, "Hybrid method to determine bus voltage and angle for line outage contingency evaluation," in *Generation, Transmission and Distribution, IEE Proceedings C*, 1992, pp. 177-184.
[20] M. Moghavvemi and F. Omar, "A line outage study for prediction of static voltage collapse," *Power Engineering Review, IEEE,* vol. 18, pp. 52-54, 1998.
[21] C. Subramani, S. Dash, M. Arun Bhaskar, M. Jagadeeshkumar, K. Sureshkumar, and R. Parthipan, "Line outage contingency screening and ranking for voltage stability assessment," in *Power Systems, 2009. ICPS'09. International Conference on*, 2009, pp. 1-5.
[22] B. Suthar and R. Balasubramanian, "A New Approach to Real Time Line Outage Contingency Analysis for Voltage Secure Operation of Power Systems," in *Power System Technology and IEEE Power India Conference, 2008. POWERCON 2008. Joint International Conference on*, 2008, pp. 1-8.
[23] *Power System Stability*. Available: http://www.electrical4u.com/power-system-stability/
[24] P. Lagonotte, J. C. Sabonnadiere, J. Y. Leost, and J. P. Paul, "Structural analysis of the electrical system: application to secondary voltage control in France," *IEEE Transactions on Power Systems,* vol. 4, pp. 479-486, 1989.
[25] M. D. Ilic and A. Chakrabortty, "Control and Optimization Methods for Electric Smart Grids," ed, p. 245.
[26] P. Kundur, N. J. Balu, and M. G. Lauby, *Power system stability and control* vol. 7: McGraw-hill New York, 1994.
[27] B. Stott and O. Alsaç, "Fast decoupled load flow," *IEEE transactions on power apparatus and systems,* pp. 859-869, 1974.
[28] A. J. Wood and B. Wollenberg, "Power generation operation and control—2nd edition," in *Fuel and Energy Abstracts*, 1996, pp. 410-432.
[29] S. E. G. Mohamed, A. Y. Mohamed, and Y. H. Abdelrahim, "Power system contingency analysis to detect network weaknesses," in *Zaytoonah University International Engineering Conference on Design and Innovation in Infrastructure, Amman, Jordan, pp. I3-4 Jun*, 2012.
[30] A. J. Wood and B. F. Wollenberg, *Power generation, operation, and control*: John Wiley & Sons, 2012.
[31] *IEEE 118-Bus System*. Available: http://icseg.iti.illinois.edu/ieee-118-bus-system/
[32] V. Centeno, J. Thorp, A. Phadke, J. De La Ree, A. Pal, M. Tania*, et al.*, "Adaptive Relay Technology Development and Measurements," Public Interest Energy Research (PIER) Program Final Project Report.
[33] M. Tania, "Wide Area Measurement Applications for Improvement of Power System Protection," 2013.